PHOTOREDOX HYDROFUNCTIONALIZATION OF ALLYLIC DIFLUORIDES

DENNIS D. TOPORKOV

An honour thesis submitted
in partial fulfilment of the requirements for the degree of

BACHELOR OF SCIENCE

in

CHEMISTRY

Department of Chemistry and Biochemistry
University of Lethbridge
LETHBRIDGE, ALBERTA, CANADA

COMMITTEE MEMBERS

Principal Investigator: Dr. Jean-Denys Hamel

Second Reader: Dr. Susan Findlay

ACKNOWLEDGEMENTS

I would like to thank J.D. for all his support, mentorship and guidance throughout my chemistry career and to thank him for his passion for organic chemistry. I would also like to thank Taylor Semeniuk for much of the same. Thank you to all other past/present group member, I could not have done it without you.

Table of Contents

List of Abbreviations

4CzIPN	2,4,5,6-tetrakis(9*H*-carbazol-9-yl) isophthalonitrile
anh.	anhydrous
Ar	aryl
Boc	*tert*-butyloxycarbonyl
bpy	2,2'-bipyridine
conc.	concentrated
DAST	diethylaminosulfur trifluoride
DCM	dichloromethane
Deoxo-Fluor	bis(2-methoxyethyl)aminosulfur trifluoride
dF(CF_3)ppy	2-(2,4-difluorophenyl)-5-(trifluoromethyl)pyridine
DIPEA	*N,N*-diisopropylethylamine
DMA	dimethylacetamide
DMAP	4-dimethylaminopyridine
DMDC	dimethyl dicarbonate
DMF	dimethylformamide
DMSO	dimethylsulfoxide
dtbbpy	4,4′-di-*tert*-butyl-2,2′-bipyridyl
Eosin Y	2',4',5',7'-tetrabromofluorescein
eq.	equivalents
Et	ethyl
EWG	electron-withdrawing group
FDA	Food and Drug Administration (USA)
H.E	Hantzsch ester
HAT	hydrogen atom transfer
HFIP	hexafluoroisopropanol
HMDS	hexamethyldisilazane
hv	Energy of a photon
IC_{50}	half-maximal inhibitory concentration
iPr	isopropyl
LED	light-emitting diode
Me	methyl
Mes-Acr	9-mesityl-10-methylacridinium perchlorate
***n*-Bu**	*n*-butyl
NHPI	*N*-hydroxyphthalimide
NMR	nuclear magnetic resonance
***n*Pr**	*n*-propyl
O/N	overnight
PC	photocatalyst
PCET	proton-coupled electron transfer
Ph	phenyl
Phth	pthalyl
pK_a	negative logarithm of the acid dissociation constant
ppm	parts per million

ppy	2-phenylpyridine
RT	room temperature
sat.	saturated
SET	single-electron transfer
SM	starting material
TFA	trifluoroacetic acid
TFE	2,2,2-trifluoroethanol
TFMA	trifluoromethylalkene
tripSH	2,4,6-triisopropylbenzenethiol
TTMSS	tris(trimethylsilyl)silane
XtalFluor-E	(diethylamino)difluorosulfonium tetrafluoroborate

1. Introduction

1.1 Organofluorine compounds

Fluorine continues to play a vital role in the advancement of synthetic methods and the development of novel molecules. Pharmaceuticals and agrochemicals, compounds that help keep the world population healthy and fed, both massively benefit from the inclusion of fluorine and its unique properties in their structures. In particular, fluorine has a higher electronegativity than other halogens and common heteroatoms in organic molecules (**Table 1**). Using the updated thermochemical scale by Tantardini and Oganov, fluorine's electronegativity (4.00) is the highest of all elements except helium and neon; similarly fluorine has the highest Pauling electronegativity (helium and neon are not given a value).[1] Additionally, fluorine has a van der Waals radius of 1.47 Å, a radius significantly smaller than most elements encountered in organic chemistry.[2] Fluorine also forms a very strong single bond with carbon (**Figure 1**).[3]

Table 1. Electronegativities and van der Waals radii of common elements in organic compounds

Element	Tantardini and Oganov Electronegativity[1]	Pauling Electronegativity ($eV^{-1/2}$)	Van der Waals radii[2] (Å)
F	4.00	3.98	1.47
Cl	3.50	3.16	1.75
Br	3.45	2.96	1.85
I	3.20	2.66	1.98
O	3.78	3.44	1.52
N	3.56	3.04	1.55
C	3.15	2.55	1.70
H	3.04	2.20	1.20

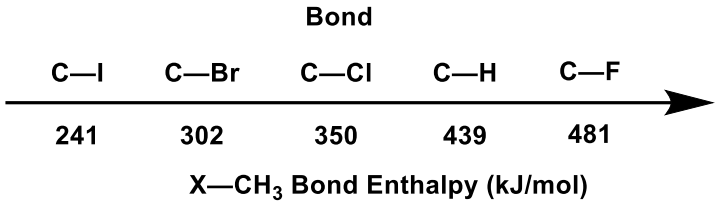

Figure 1. Comparison of bond enthalpies in CH_3X

These properties of fluorine can impart valuable characteristics to the molecules that bear it, such as enhanced binding interactions, increased metabolic stability, increased lipophilicity and more selective reactivities.[4,5] An example of the beneficial effects of fluorine substitution can be seen in amodiaquine, an anti-malaria drug (**Figure 2**).[6] Upon replacement of the hydroxyl group with a fluorine atom, the drug

maintains anti-malarial efficacy whilst becoming more resistant to *in vivo* oxidation, a process which forms toxic metabolites.

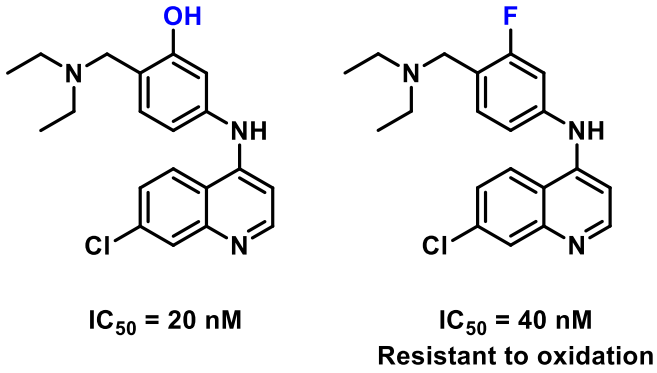

Figure 2. Anti-malaria drug amodiaquine (left) and a fluorinated derivative (right)

Between 2018 and 2025, a total of 252 small molecule drugs were approved by the FDA.[7-14] Among these, 91 (36%) contained at least one fluorine atom (**Table 2**). Some examples include suzetrigine, a $Na_V1.8$ blocker, inavolisib, a treatment for breast cancer, and nirmatrelvir, one of the two major components of Paxlovid™, an oral anti-viral to treat coronavirus (**Figure 3**).[15-17]

Table 2. Number of small molecule FDA-approved drugs with at least 1 fluorine atom, 2018-2025

Year	Total Drugs (small molecule)	Fluorine-containing Drugs	% Fluorinated
2018	38	17	45
2019	33	11	33
2020	34	13	38
2021	33	9	27
2022	22	4	18
2023	32	12	38
2024	31	11	35
2025	29	14	48
Total	252	91	36

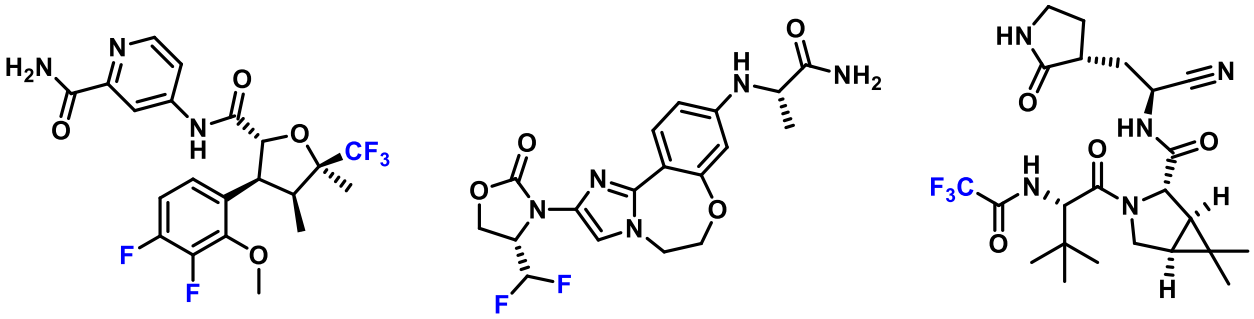

Figure 3. Examples of fluorine-containing pharmaceuticals, with year of FDA approval

Similarly, agrochemicals have often benefitted from the inclusion of fluorine. In 2003, it was reported that 16% of known agrochemicals were fluorinated molecules. An analysis done between 1998 and 2020 showed that 53% of all agrochemicals were fluorinated molecules, showing a dramatic increase in the proportion of fluorinated agrochemicals.[18] Fluorine has made substantial contributions to both the pharmaceutical and agrochemical industries, with increasing numbers of molecules bearing fluorine appearing in literature, likely supported by new and improved methodologies emerging. Among the fluorinated molecules compiled in Table 2, a majority of them feature mono- and trifluorination. Similarly, a survey was conducted which compiled fluorine-containing pesticides including insecticides, herbicides, fungicides and other similar compounds from several pesticide databases and patent searches.[18] Of the 424 fluoroagrochemicals identified, mono- and trifluorinated molecules accounted for a combined 77% of the total compounds. However, the -CF_2- group still proves to be a useful moiety, featuring in 11/91 (12%) of the fluorinated drugs from Table 2 and in 27/424 (6%) of agrochemicals emerging from the survey, such as cedazuridine and quinofumelin (**Figure 4**).[18]

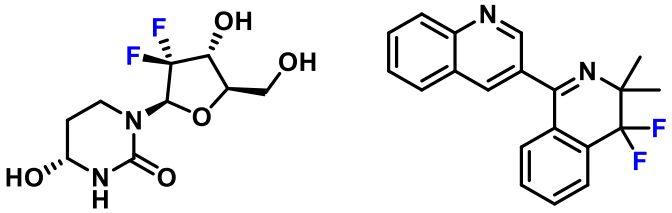

Figure 4. Two compounds with *gem*-difluoro groups. Cedazuridine is used to treat myelodysplastic syndromes and leukemia.[19] Quinofumelin is a fungicide against *Fusarium graminearum*.[20]

Thus, there is a desire to synthesize molecules bearing *gem*-difluoro groups, ideally from readily available functional groups such as carbonyl compounds. A breakdown of types of -CF_2- moieties seen in the 11 FDA-approved drugs featuring *gem*-difluorination reveals the most common grouping has two alkyl groups bonded to the difluoromethylene (**Figure 5**).

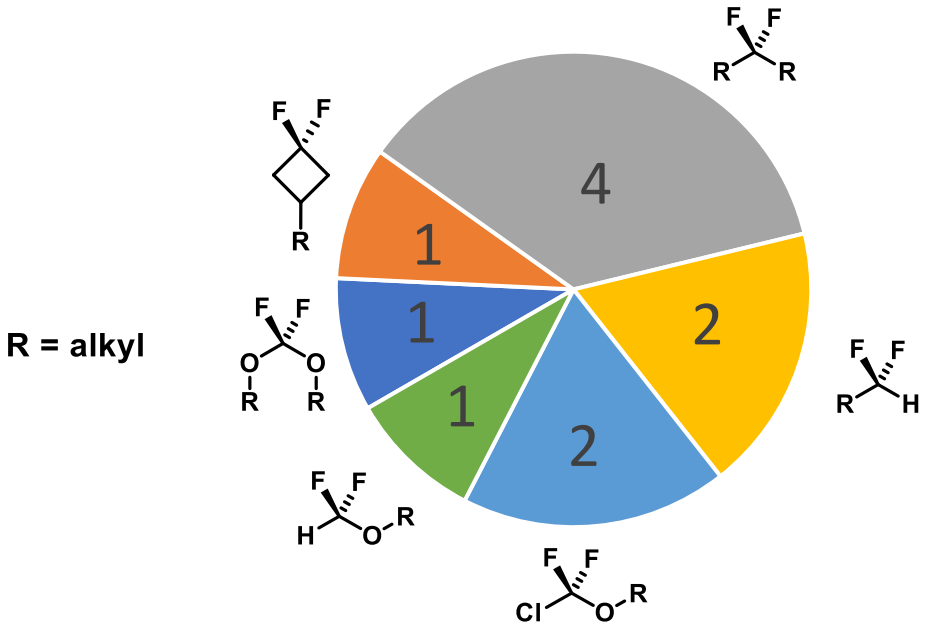

Figure 5. Breakdown of *gem*-difluoro groups seen in the 11 FDA-approved *gem*-difluorinated drugs, 2018-2025

1.2 Difluorination of carbonyl compounds

As early as 1960, SF_4 was utilized to perform deoxofluorinations which, when applied to a ketone or aldehyde, generated a *gem*-difluoro group in place of the carbonyl (**Scheme 1**); however, SF_4 is a highly toxic gas and requires substantial safety precautions (**Figure 6**).[21,22] DAST was later developed as a better alternative since its liquid state enables easier handling. Unfortunately, while still being extensively used to this day, DAST is explosive and releases HF upon hydrolysis, which leads to conditions that are hazardous and incompatible with many functional groups.[23] Deoxo-Fluor was found to be more thermally stable than DAST, but still produces toxic and corrosive HF via hydrolysis.[24] Dialkylaminodifluorosulfinium tetraborate salts have also been shown to deoxofluorinate ketones and aldehydes. Specifically, diethylaminodifluorosulfonium tetrafluoroborate, also known as XtalFluor-E, has been used to perform deoxofluorination reactions, with benefits over DAST and Deoxo-Fluor including easier handling, increased

thermal stability, greater selectivity and lack of free HF generation.[22] Additionally, to perform a deoxofluorination with XtalFluor-E, an exogenous source of fluoride is required such as $Et_3N{\cdot}3HF$, a reagent less corrosive than free HF and nearly pH neutral.[25] The aforementioned methods, however, lead to undesirable mixtures of mono- and difluorinated products which are frequently difficult to separate (**Scheme 1**).[26]

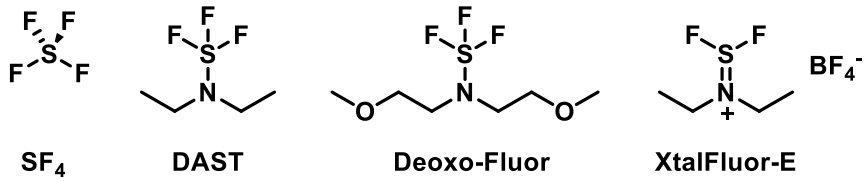

Figure 6. Several nucleophilic fluorination agents

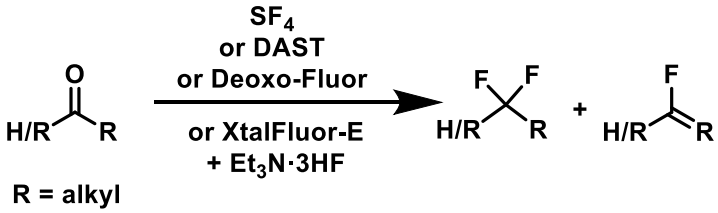

Scheme 1. Mono- and difluorination using several deoxofluorination agents

Another class of fluorinating reagents is seen with electrophilic fluorine sources, also colloquially referred to as sources of F^+. Traditional reagents such as fluorine gas, hypofluorites, fluoroxysulfates and perchloryl fluoride are highly reactive and challenging to work with. XeF_2 was developed as a more stable option but still suffers from a high oxidation potential which lowers functional group tolerance.[27] Subsequently, a variety of benchtop-stable and solid electrophilic fluorine sources were developed, including *N*-fluoropyridinium salts (such as *N*-fluoropyridinium triflate), NFSI, and Selectfluor (**Figure 7**).[28-30] Other methods to achieve *gem*-difluorination include the use of difluorocarbene precursors, metal-based compounds such as ($Zn(SO_2CF_2H)$, as well as various electrochemical and photochemical processes.[31-34]

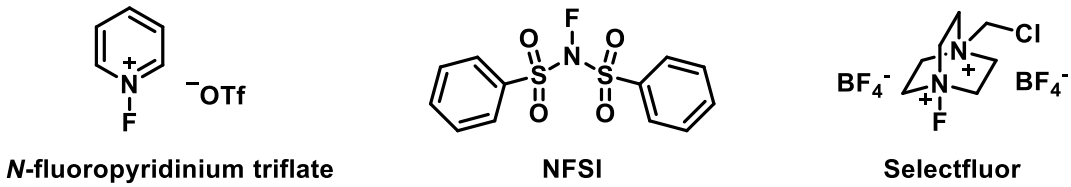

***N*-fluoropyridinium triflate** **NFSI** **Selectfluor**

Figure 7. Several electrophilic fluorination agents

When using electrophilic fluorination reagents to synthesize α,α-difluoroketones, the ketone must first be converted to an imine as monocarbonyl compounds tend to undergo monofluorination.[35] For example, the commercially available α-tetralone undergoes imine formation with *n*-butylamine catalyzed by TFA. This process is efficient enough that no further purification other than a simple aqueous work-up is required, and the imine can be subsequently fluorinated with an electrophilic fluorine source followed by hydrolysis with aqueous HCl. Under optimized conditions using anhydrous acetonitrile as the solvent, difluorination is heavily favoured, which improves yields and greatly simplifies purification (**Scheme 2**).[35] This method affords the target difluoride α to a carbonyl, but what if there is a desire to remove the carbonyl due to its reactivity? This can be accomplished using the well-known Wittig olefination reaction which, when applied to α,α-difluoroketone **1,** generates allylic difluoride **2**.[36] Crystals of the difluoroketone (**1**) were grown via evaporation of hexanes at 2-8 °C and, the resulting colourless, thin, needle-like crystals were analyzed using single-crystal X-ray diffraction. Notably, the two C-F bonds had significantly different lengths. Full crystallographic results are reported in section **5**.

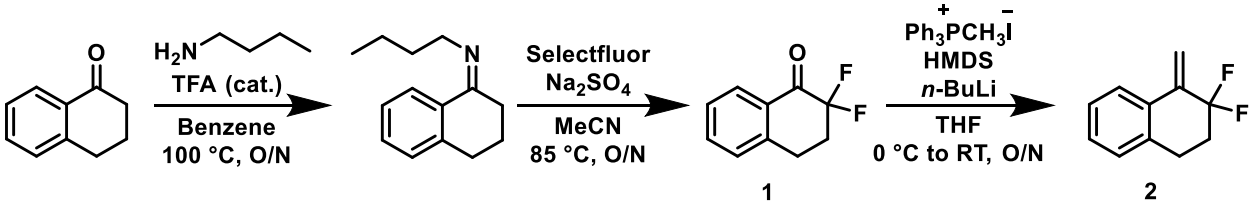

Scheme 2. The synthesis of allylic difluoride **2** from α-tetralone

1.3 Modification of allylic difluorides

Allylic difluorides are useful synthetic handles to further functionalize molecules. Monofluoroalkenes are popular motifs in the pharmaceutical industry as they can act as amide bioisosteres and enol mimics (**Figure 8**).[37] Methods to generate monofluoroalkenes from allylic difluorides include the use of organolithium reagents as well as several methods that feature transition metal catalysis with Pd, Pt or Rh/Ag.[38-41] Another method, developed by the Hamel group, features photoredox catalysis using Ir and Rh-based catalysts enabling the addition of acyl or alkyl radicals, followed by β-fluoride elimination which affords functionalized monofluoroalkenes.[36, 42] This process was found to be amenable to organophotocatalysis, resulting in metal-free conditions.[43]

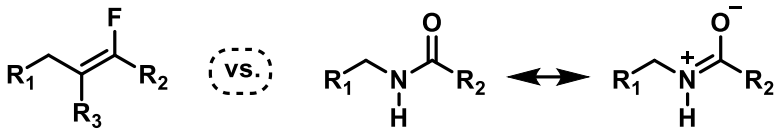

Figure 8. Comparison between a monofluoroalkene and a generalized peptide fragment

Due to the appeal of *gem*-difluoro compounds, there was a desire to retain both fluorine atoms in radical-based reactions of allylic difluorides. It was hypothesized that allylic difluorides could be hydrofunctionalized photocatalytically, thereby retaining the *gem*-difluoro group while removing the alkene. The challenge lays in overriding previous efforts to favour β-fluoride elimination, a process which has proven to be efficient for allylic difluorides via photoredox methods, by promoting an orthogonal hydrofunctionalization pathway (**Scheme 3**). Theoretically, hydrofunctionalization could proceed via a purely radical mechanism where an H· is abstracted from a hydrogen atom donor by the generated carbon-centered radical. Alternatively, the radical may be reduced via single-electron transfer (SET), producing a carbanion which could then be protonated.

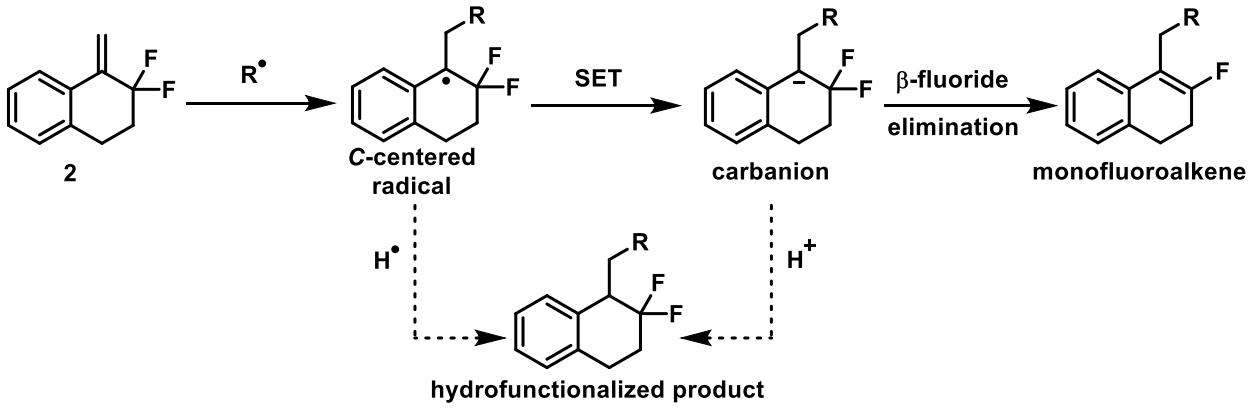

Scheme 3. The conversion of allylic difluoride **1** into its corresponding monofluoroalkene and proposed orthogonal pathways to hydrofunctionalized products.

A literature search was conducted, focusing on the hydrofunctionalization of groups structurally similar to allylic difluorides such as trifluoromethylalkenes (TFMAs) and, more generally, alkenes attached to electron-withdrawing groups (EWGs). Several methodologies, particularly those featuring photoredox catalysis, have been developed to achieve hydrofunctionalization of alkenes, especially those bonded to EWGs.[44-46] Of particular interest are carboxylic acids, *N*-hydroxyphthalimide (NHPI) esters, *N*-heterocycles,

aldehydes and alkanes. Carboxylic acids and their derivatives, such as α-ketoacids, can acylate electron-poor alkenes.[45, 46] Carboxylic acids can also easily be converted into NHPI esters which can then alkylate groups of interest onto electron-poor alkenes.[47-49] Similarly, halopyridines and diazines have been used to hydrofunctionalize electron-poor alkenes.[50] Aldehydes and alkanes can also be used as radical precursors to acylate and alkylate, respectively; however, those methods require UV light, whereas the methods for the other precursors mentioned above use blue or green light.[51-53] Due to time constraints, this work will focus on carboxylic acid, NHPI ester and *N*-heterocycle radical precursors. Besides achieving desired reactivity, carboxylic acids are commercially abundant and cheap materials.[54] *N*-Heterocycles are also important groups for agrochemicals; it is estimated that more than 70% of agrochemicals contain a heterocycle, commonly an *N*-heterocycle.[18] Additionally, from the 424 fluoroagrochemicals aforementioned (Section 1.1), 259 (61%) of them contain fluorine and an *N*-heterocycle.[18] Furthermore, a reported 60% of FDA-approved drugs contain *N*-heterocycles.[55]

Previous work done by the Hamel group has demonstrated the photocatalytic transformation of allylic difluorides to monofluoroalkenes utilizing both metal-based and organic photocatalysts (**Scheme 4**).[36, 42, 43, 56] The photochemical pathways developed favour β-fluoride elimination using radical precursors such as carboxylic acids, α-ketoacids and *N*-alkylanilines.

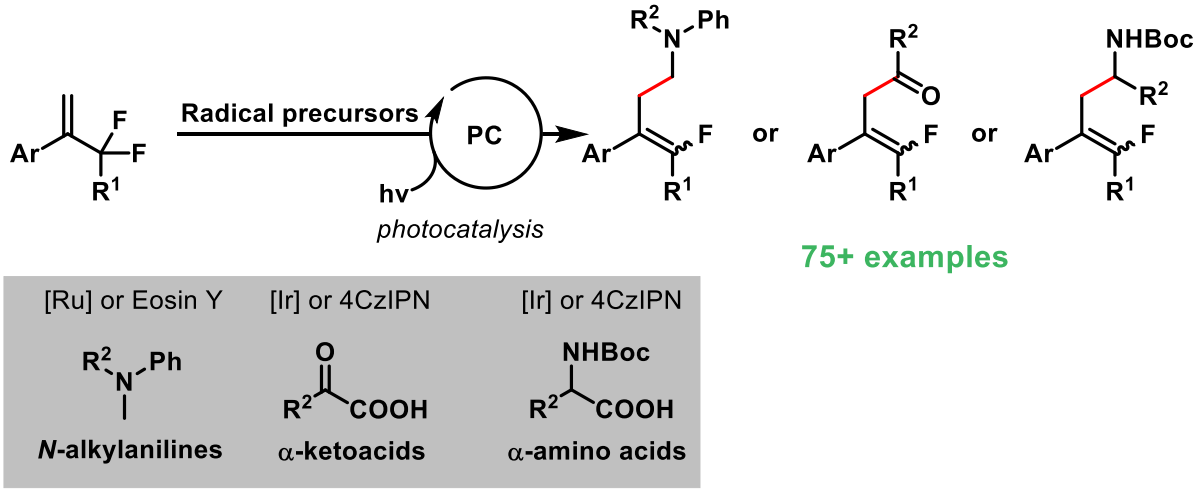

Scheme 4. Photoredox synthesis of monofluoroalkenes from allylic difluorides

2. Methodology

The alkylation of alkenes with NHPI esters is known to occur without the use of a photocatalyst, while using Hantzsch esters (H.E, **Figure 9**) which form electron donor-acceptor complexes *in situ*.[48, 49] Hantzsch esters are also sources for single-electron transfer (SET) and hydrogen atom transfer (HAT) which promote the formation of hydrofunctionalized product. Other methods have had success using dual-solvent organic/water systems, as H_2O can act as a hydrogen source which can promote hydrofunctionalization.[44, 45, 50] In general, initial optimization conditions in each case were based on known examples of hydrofunctionalization of TFMAs or other electron-poor alkenes.

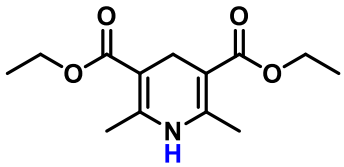

Hantzsch ester

Figure 9. Structure of the Hantzsch ester

The alkylation of TFMAs from NHPI esters is known and utilizes the Hantzsch ester as both a hydrogen source and a photocatalyst (**Scheme 5**).[48] This photocatalytic activity is achieved by the formation of an electron donor-acceptor complex *in situ* between the NHPI ester and the Hantzsch ester. It was correctly suspected that a photocatalyst would be necessary to achieve the desired result as the power of the LEDs used in the literature case is much higher than currently available to us (24 W vs 16 W). **Method A** refers to conditions based on literature (no additional photocatalyst), and **Method B** refers to the same conditions with an added photocatalyst.

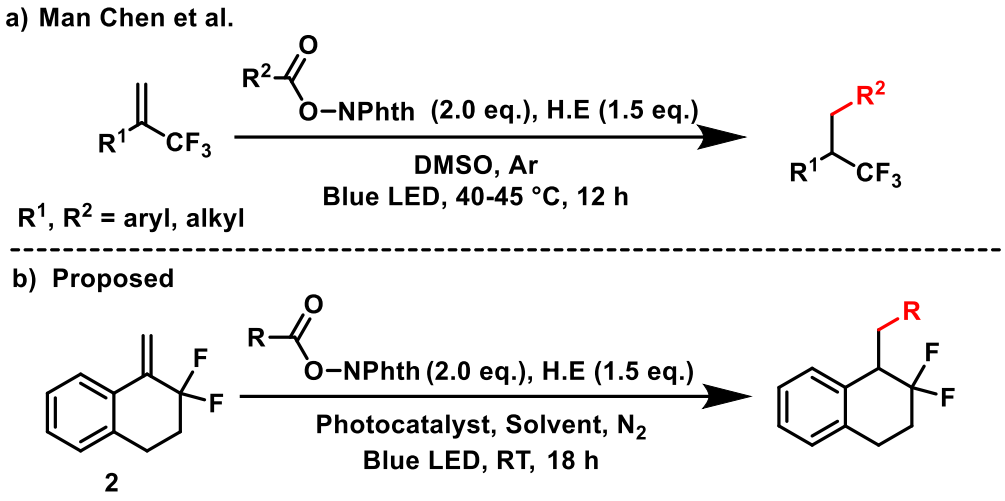

Scheme 5. a) Hydroalkylation of TFMAs with NHPI esters[48] and b) proposed hydroalkylation of allylic difluoride **2** under analogous conditions (**Methods A/B**)

Another method achieves arylation of electron-poor alkenes with NHPI esters with the benefit of a green photocatalyst, in contrast to commonly employed metal photocatalysts, whilst being reportedly not air-sensitive. Since there was no product formation, the air-sensitivity is unconfirmed. Interestingly, DIPEA acts as the hydrogen source as well as a base in this system (**Scheme 6**).[47] This method is referred to as **Method C** in this manuscript.

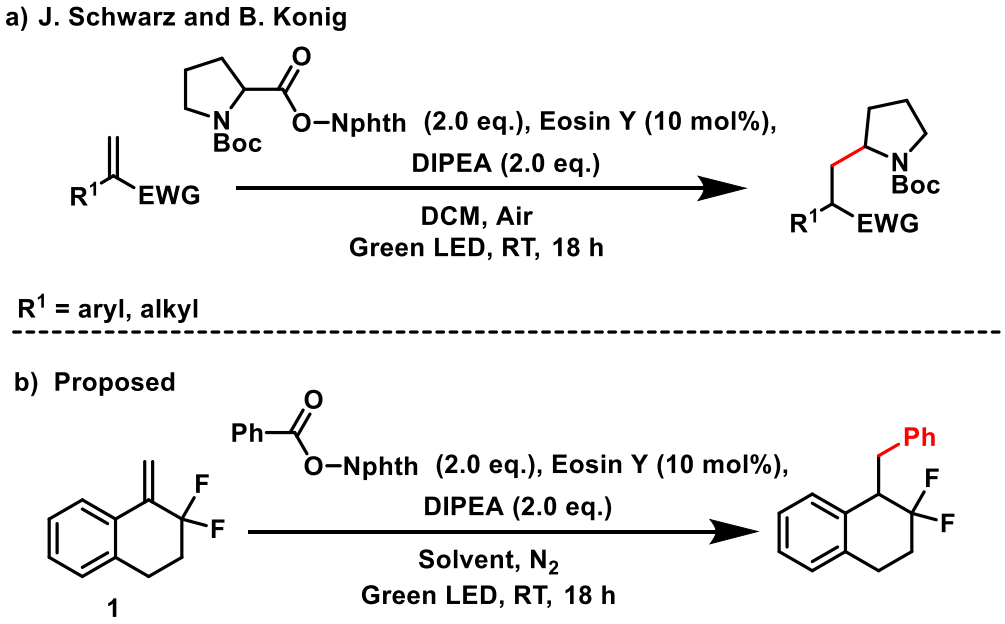

Scheme 6. a) Hydroaminoalkylation of electron-deficient alkenes[47] and b) proposed hydroarylation of allylic difluoride **2** under analogous conditions (**Method C**)

The acylation of TFMAs with carboxylic acids is known (**Scheme 7**). The formation of triphenylphosphine oxide drives the reaction, enabling direct acylation, as opposed to alkylation with NHPI esters.[44] This method is referred to as **Method D**.

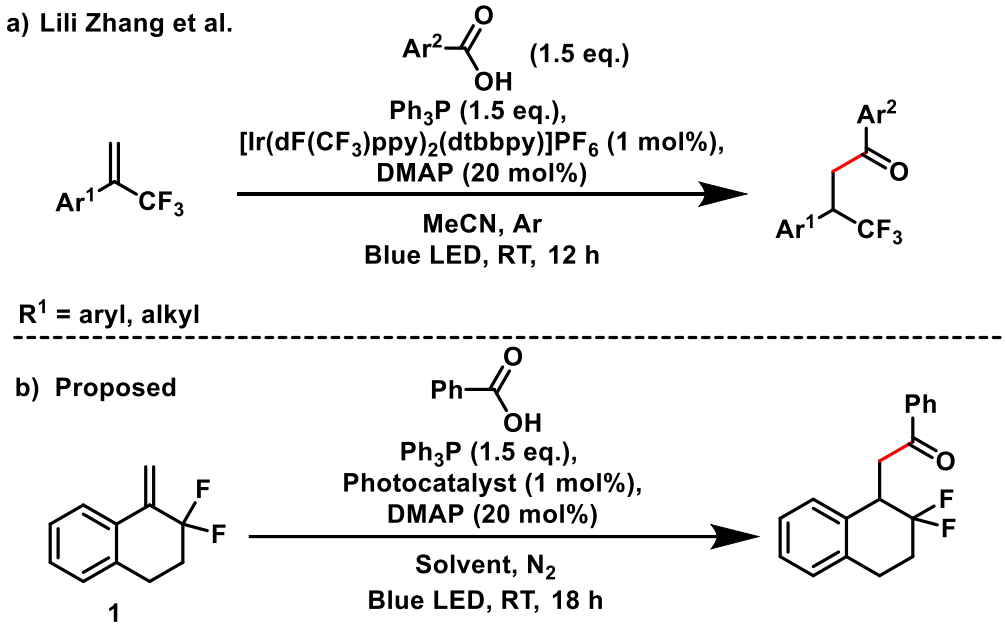

Scheme 7. a) Hydroacylation of TFMAs[44] and b) proposed hydroacylation of allylic difluoride **2** under analogous conditions (**Method D**)

The heteroarylation of electron-poor alkenes has been performed using iodo- and bromopyridines and their derivatives (**Scheme 8**). This method is referred to as **Method E**. Halogenated diazines have also been successfully employed in this transformation (**Figure 10**).[50]

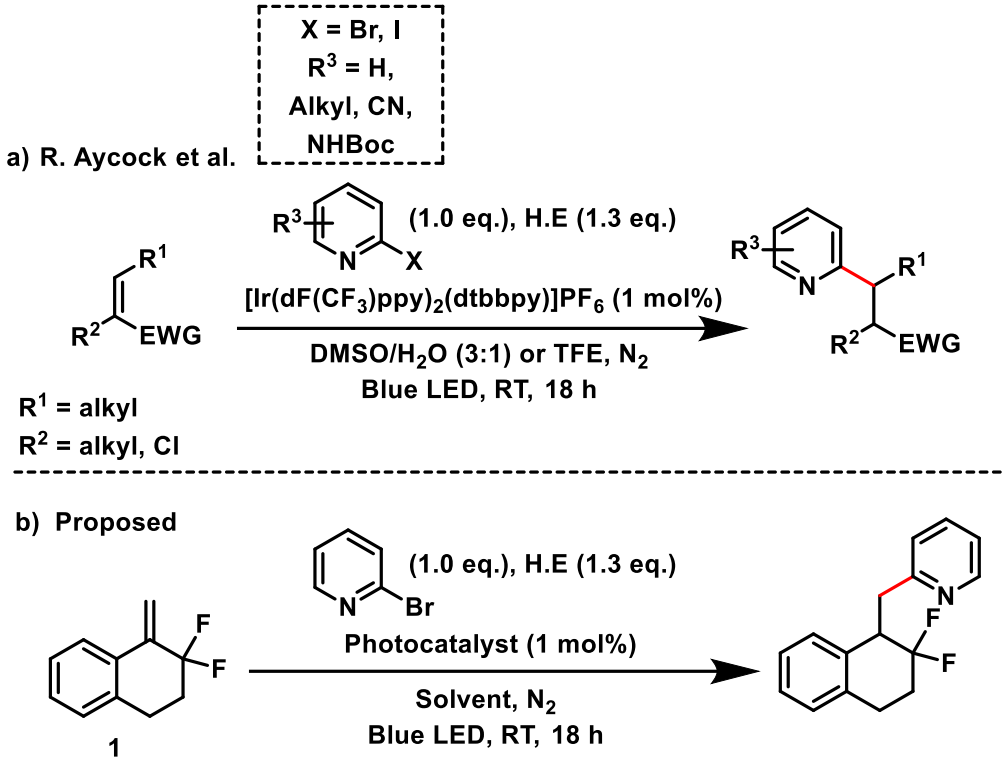

Scheme 8. a) Hydroheteroarylation of electron-deficient alkenes[50, 57] and b) proposed hydroheteroarylation of allylic difluoride **2** under analogous conditions (**Method E**)

Figure 10. Examples of diazines used in the hydroheteroarylation of electron-poor alkenes

3. Results and Discussion

3.1 Initial optimization

Initial rounds of optimization sought to test a small number of reactions with different methods and radical precursors, with the goal of identifying the most promising combination, as time limitations prevented thorough optimization of multiple systems. Methods were executed as discussed in the methodology section, with solvent optimization as the focus. Subsequent optimization involved photocatalyst optimization, the selection of which was based on half-reduction oxidation/reduction potentials (**Figure 12**). Throughout the optimization process, yield was monitored using ^{19}F and $^{19}F\{^{1}H\}$ NMR spectroscopy, enabling faster

reaction screening by mitigating the need for solvent evaporation and purification. Based on several representative structures, it was predicted that, the $^{19}F\{^{1}H\}$ NMR spectra would feature a doublet for each geminal fluorine in roughly the -90 ppm to -110 ppm region, each with a coupling constant of roughly $^{2}J_{FF}$ = 240 – 250 Hz (**Figure 11**).[58] In the ^{19}F NMR spectrum, it was expected that two doublet of doublet of doublet of doublets (dddd) will be observed given high enough resolution, when assuming non-zero $^{3}J_{HF}$ coupling constants.

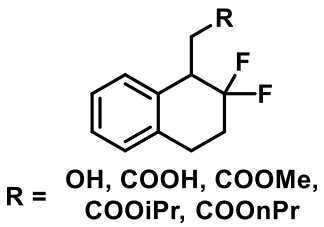

Figure 11. Representative 2,2-difluoro-1,2,3,4-tetrahydronapthalene molecules[58]

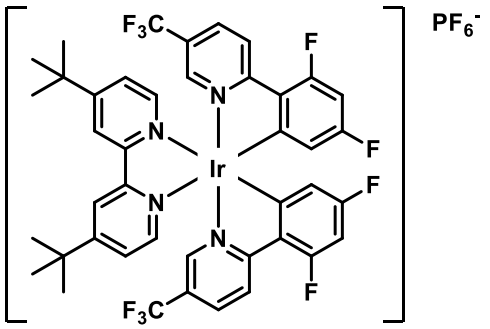

[Ir{dF(CF$_3$)ppy}$_2$(dtbbpy)][PF$_6$] = [Ir]CF$_3$
$E_{1/2}$(PC*/PC$^-$) = +1.21 V
$E_{1/2}$(PC/PC$^-$) = -1.37 V

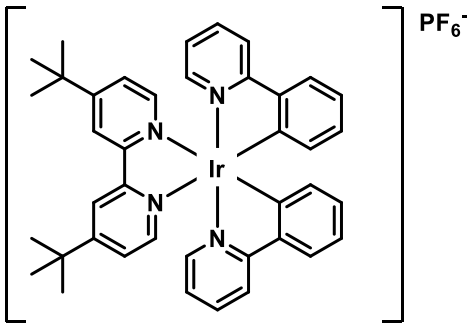

[Ir(ppy)$_2$(dtbbpy)][PF$_6$] = [Ir]ppy$_2$
$E_{1/2}$(PC*/PC$^-$) = +0.66 V
$E_{1/2}$(PC/PC$^-$) = -1.51 V

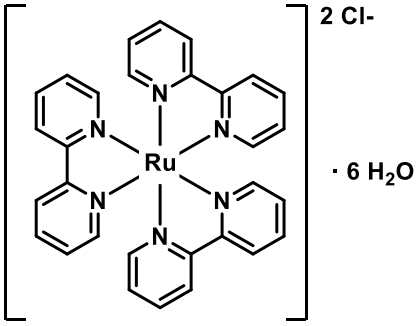

[Ru(bpy)$_3$][Cl$_2$]·6H$_2$O = [Ru]E
$_{1/2}$(PC*/PC$^-$) = +0.77 VE
$_{1/2}$(PC/PC$^-$) = -1.33 V

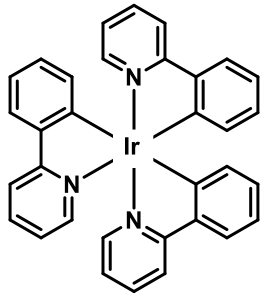

Ir(ppy)$_3$
$E_{1/2}$(PC*/PC$^-$) = +0.31 V
$E_{1/2}$(PC/PC$^-$) = -2.19 V

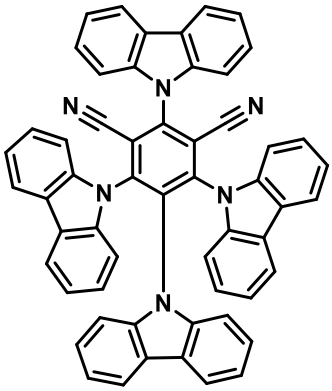

4CzIPN
$E_{1/2}$(PC*/PC$^-$) = +1.43 V
$E_{1/2}$(PC/PC$^-$) = -1.24 V

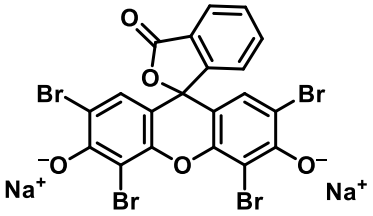

Eosin Y
$E_{1/2}$(PC*/PC$^-$) = +0.83 V
$E_{1/2}$(PC/PC$^-$) = -1.06 V

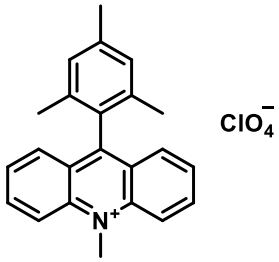

9-mesityl-10-methylacridinium perchlorate = Mes-Acr
$E_{1/2}$(PC*/PC$^-$) = +2.06 V
$E_{1/2}$(PC/PC$^-$) = -0.57 V

Figure 12. Photocatalysts used in optimization, with half-reduction potentials (abbreviations in blue)

Upon analysis of initial results, two sets of peaks matching the above description were identified. It appeared that two products were present, both with very similar chemical shifts, multiplicities and coupling constants; both matched expected values for the product. This was observed with the radical precursors 1,3-dioxoisoindolin-2-yl benzoate (**Table 3, entries 2, 5 and 8**) and 2-bromopyridine (**entries 17-20**). To keep track of the two sets of products, they have been designated as "A" and "B" for the products generated from 1,3-dioxoisoindolin-2-yl benzoate, "C" and "D" for the products generated from benzoic acid and "X" and "Y" for products generated from 2-bromopyridine.

From among the results seen in Table 3, it was clear methods B and E were most promising; however, method E was best with three out of four results yielding 13-17% (**entries 17-20**). Method E also consistently had the best starting material conversion when compared to other methods. For this reason, Method E was chosen as the main reaction system to optimize further.

Table 3. Initial optimization results, Methods A-E are described in section 2.0[a]

Method A[b] Entry	**Solvent**	**Photocatalyst**	**SM Conversion (%)**	**Yield A (%)**	**Yield B (%)**	**A+B (%)**
1	DMF	None	21	0	0	0
2	DMA	None	88	3	4	7
3	DCM	None	21	0	0	0
4	MeCN	None	40	0	0	0
Method B[c] Entry	**Solvent**	**Photocatalyst**	**SM Conversion (%)**	**Yield A (%)**	**Yield B (%)**	**A+B (%)**
5	DMA	$[Ir]CF_3$	100	8	7	15
6	MeCN/H_2O (3:1)	$[Ir]CF_3$	72	0	0	0
7	MeCN	$[Ir]CF_3$	59	0	0	0
8	DMF	$[Ir]CF_3$	73	3	3	6
Method C[d] Entry	**Solvent**	**Photocatalyst**	**SM Conversion (%)**	**Yield A (%)**	**Yield B (%)**	**A+B (%)**
9	DMF	Eosin Y	16	0	0	0
10	DMA	Eosin Y	68	0	0	0
11	DCE	Eosin Y	13	0	0	0
12	MeCN	Eosin Y	2	0	0	0
Method D[e] Entry	**Solvent**	**Photocatalyst**	**SM Conversion (%)**	**Yield C (%)**	**Yield D (%)**	**C+D (%)**
13	MeCN	$[Ir]CF_3$	100	0	0	0
14	DCM	$[Ir]CF_3$	64	0	0	0

15	DMF	[Ir]CF_3	53	0	0	0
16	DCM:H_2O (4:1)	[Ir]CF_3	99.9	0	0	0
Method E[f] Entry	**Solvent**	**Photocatalyst**	**SM Conversion (%)**	**Yield X (%)**	**Yield Y (%)**	**X+Y (%)**
17	MeCN/H_2O (3:1)	[Ir]CF_3	100	5	10	15
18	DMF/H_2O (3:1)	[Ir]CF_3	100	7	6	13
19	MeOH/H_2O (3:1)	[Ir]CF_3	100	4	13	17
20	DMSO/H_2O (3:1)	[Ir]CF_3	100	Trace	Trace	Trace

[a]General Conditions: allylic difluoride **1** (0.2000 mmol), 2 mL solvent, N_2,18 h

[b]Conditions: 1,3-dioxoisoindolin-2-yl benzoate (0.4000 mmol), Hantzsch Ester (0.3000 mmol), blue light (465 nm)

[c]Conditions: benzoic acid (0.2200 mmol), PPh_3 (0.3000 mmol), DMAP (0.0400), (Ir[dF(CF_3)ppy]$_2$(dtbbpy))PF_6 (0.0020 mmol), blue light (465 nm)

[d]Conditions: 1,3-dioxoisoindolin-2-yl benzoate (0.4000 mmol), Hantzsch Ester (0.3000 mmol), (Ir[dF(CF_3)ppy]$_2$(dtbbpy))PF_6 (0.0020 mmol), blue light (465 nm)

[e]Conditions: 1,3-dioxoisoindolin-2-yl benzoate (0.4000 mmol), DIPEA (0.400 mmol), Eosin Y (0.0200 mmol), green light (530 nm)

[f]Conditions: 2-bromopyridine (0.400 mmol), Hantzsch Ester (0.2600 mmol), (Ir[dF(CF_3)ppy]$_2$(dtbbpy))PF_6, blue light (465 nm)

3.2 Further optimization

Utilizing the method with the most promising results, the optimization of the *N*-heteroarylation of allylic difluoride **2** with 2-bromopyridine as a model substrate was attempted. A series of solvents were tested, including dual solvent systems with H_2O and TFE, both of which have shown to give good results in the heteroarylation of alkene substrates (**Table 4**).[59] The dual MeOH/H_2O solvent (entry 19) provided the best results. A common and quite high yielding impurity appears at about -103.0 ppm to -103.1 ppm in the ^{19}F NMR spectrum, which matches expected values for monofluoroalkenes. This is logical as the formation of monofluoroalkenes was initially identified as a main competing pathway (**Scheme 3**). Notably, entries 18 and 20 saw suspected monofluoroalkene production in yields of 39% and 32%, respectively. This corroborates the theory that the recurring impurity at roughly -103 ppm is the monofluoroalkene product as DMF and DMSO were previously shown to effectively generate monofluoroalkenes from allylic difluoride **2** with α-ketoacids, α-amino acids and *N*-alkylanilines.[36, 42, 56]

Table 4. Solvent optimization for the heteroarylation of allylic difluoride **2**

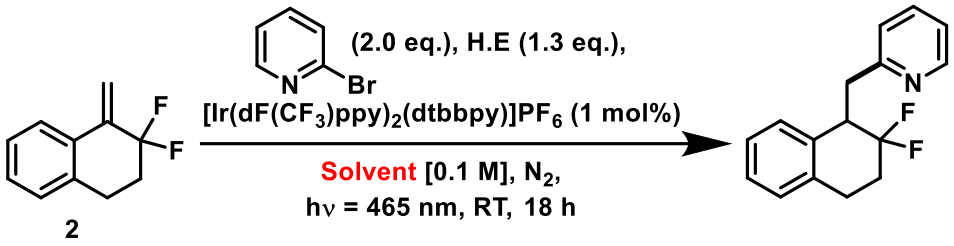

2

Entry	Solvent	SM Conversion (%)	Yield X (%)	Yield Y (%)	X+Y (%)
1	MeCN/H_2O (3:1)	100	5	10	15
2	DMF/H_2O (3:1)	100	7	6	13
3	MeOH/H_2O (3:1)	100	4	13	17
4	DMSO/H_2O (3:1)	100	Trace	Trace	Trace
5	DMA/H_2O (3:1)	100	0	0	0
6	DMA	100	0	0	0
7	MeOH	100	Trace	Trace	Trace
8	HFIP	100	0	0	0
9	TFE	96	Trace	Trace	Trace

4CzIPN is a purely organic photocatalyst which has shown to be capable of transforming allylic difluorides into monofluoroalkenes as an alternative to the metal-based (Ir[dF(CF_3)ppy]$_2$(dtbbpy))PF_6.[60] 4CzIPN achieves comparable yields and is greener and more cost-effective than the original photocatalyst. For this reason, it was chosen for the next set of optimization reactions (**Table 5, entries 1-6**). Initially, 4CzIPN had low conversion in MeOH/H_2O; HFIP and TFE improved conversion but lowered yields. Interestingly, adding NH_4Cl, a weak acid (pK_a = 9.24), to the reaction in TFE increased yield while maintaining nearly the same conversion. Next, the conversion of entry 1 was improved by increasing the photocatalyst load to 3 mol% (entry 5) and by doubling the solution concentration (entry 6). Both changes increased conversion to 100% and MeOH/H_2O continued to be the best performing solvent system. Next, several photocatalysts were tested, namely [Ir(ppy)$_2$dtbbpy]PF_6, Ru(bpy)$_3Cl_2 \cdot 6H_2O$, Ir(ppy$_3$), Eosin Y and [Ir(dF(CF_3)ppy$_2$)(dtbbpy)]PF_6. Entries 5 and 7 utilizing [Ir(ppy)$_2$dtbbpy]PF_6 and 4CzIPN as the photocatalysts gave the best results.

Table 5. Photocatalyst and further solvent optimization

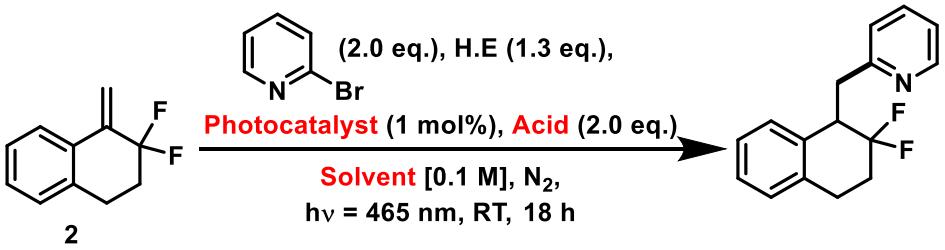

2

Entry	Solvent	Photocatalyst	Acid Additive	SM Conversion (%)	Yield X (%)	Yield Y (%)	X+Y (%)
1	MeOH/H_2O (3:1)	4CzIPN	None	54	3	2	5
2	HFIP	4CzIPN	None	89	0	0	0
3	TFE	4CzIPN	None	80	1	1	2
4	TFE	4CzIPN	NH_4Cl	81	6	6	11
5[a]	MeOH/H_2O (3:1)	4CzIPN	NH_4Cl	100	8	7	15
6[b]	MeOH/H_2O (3:1)	4CzIPN	NH_4Cl	100	6	7	13
7	MeOH/H_2O (3:1)	[Ir]ppy_2	NH_4Cl	100	6	12	17
8	MeOH/H_2O (3:1)	[Ru]	NH_4Cl	68	4	5	10
9	MeOH/H_2O (3:1)	$Ir(ppy)_3$	NH_4Cl	8	0	0	0
10[c]	MeOH/H_2O (3:1)	Eosin Y	NH_4Cl	1	0	0	0

[a]3 mol% cat. loading

[b][0.2M]

[c]10 mol% cat. Loading, hv = 530 nm

An acid test was performed to determine the effect of acidity on reaction success along with evaluating a HAT transfer catalyst (**Table 6**). Thiols have been shown to catalyze hydrogen atom transfer which could sufficiently speed up H· abstraction to potentially avoid SET and subsequent β-F elimination.[50, 61] 2,4,6-Triisopropylbenzenethiol (tripSH) was utilized and upon comparing entry 1 in Table 6 and entry 7 in Table 5, there is a marginal increase in yield at a lower conversion. Considering NMR error (±3%), this improvement is negligible; however, it is not a detriment and subsequent reactions incorporated 2,4,6-triisopropylbenzenethiol to explore its potentially beneficial effects. The reaction appears insensitive to pK_a adjustment except for the strongest tested acid TFA (pK_a = 0.23), giving similar yields in the pK_a range 9.24-2.86. As such, ammonium chloride continued to be used for its ease of handling and mild reactivity.

Table 6. Acid additive optimization

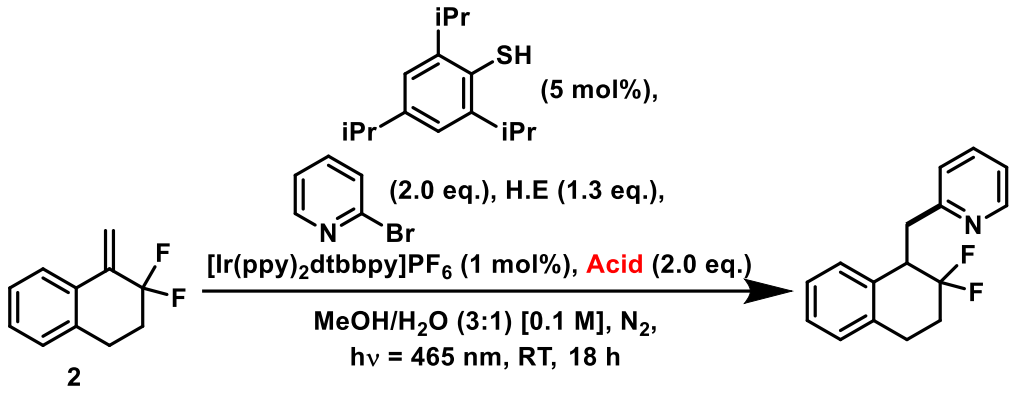

2

Entry	Acid Additive	pK_a	SM Conversion (%)	Yield X (%)	Yield Y (%)	X+Y (%)
1	NH_4Cl	9.24	86	5	13	18
2	$NaH_2PO_{4\ (anh.)}$	7.21	99	5	12	17
3	acetic acid	4.76	98	7	12	20
4	chloroacetic acid	2.86	99	5	12	17
5	TFA	0.23	100	0	0	0

With the introduction of the HAT catalyst, photocatalysts from Table 5 were retested except for $Ir(ppy)_3$ and Eosin Y and with the addition of 9-mesityl-10-methylacridinium perchlorate (**Table 7**). Photocatalysts were tested in MeOH/H_2O (3:1) and DMSO/HFIP (9:1). DMSO is typically useful for radical processes as it is relatively inert and highly polar, whereas the addition of HFIP increases polarity to a greater extent and HFIP itself can act as an H-source that is less nucleophilic than methanol.[62] MeOH/H_2O remained the best solvent whilst both $[Ir(ppy)_2dtbbpy]PF_6$ and $[Ir(dF(CF_3)ppy_2)(dtbbpy)]PF_6$ performed comparably. $[Ir(ppy)_2dtbbpy]PF_6$ was ultimately chosen as, generally, $[Ir(dF(CF_3)ppy_2)(dtbbpy)]PF_6$ generated a greater number of fluorinated impurities.

Table 7. Photocatalyst re-screening

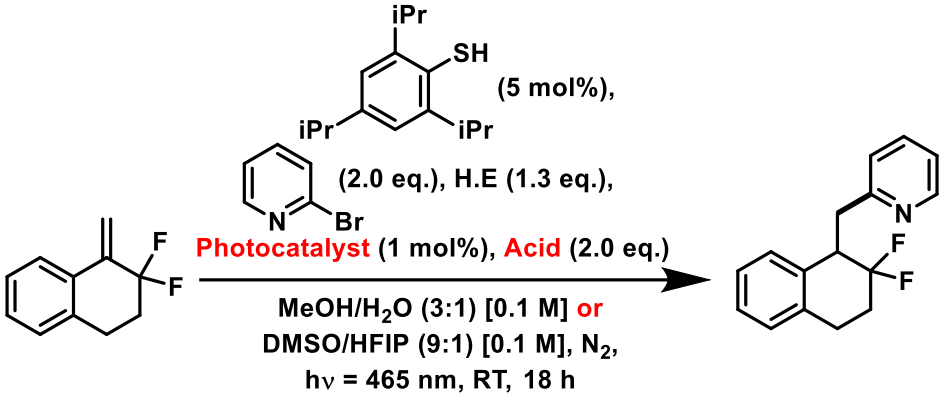

Entry	Solvent	Photocatalyst	Acid	SM Conversion (%)	Yield X (%)	Yield Y (%)	X+Y (%)
1	MeOH/H_2O (3:1)	[Ir]ppy_2	NH_4Cl	86	5	13	18
2	DMSO/HFIP (9:1)	[Ir]ppy_2	None	94	trace	trace	trace
3	MeOH/H_2O (3:1)	[Ir]CF_3	NH_4Cl	99	5	14	19
4	DMSO/HFIP (9:1)	[Ir]CF_3	None	93	trace	trace	trace
5	MeOH/H_2O (3:1)	[Ru]	NH_4Cl	99	0	0	0
6	DMSO/HFIP (9:1)	[Ru]	None	86	0	0	0
7	MeOH/H_2O (3:1)	Mes-Acr	NH_4Cl	28	0	0	0
8	DMSO/HFIP (9:1)	Mes-Acr	None	48	4	0	4
9	MeOH/H_2O (3:1)	4CzIPN	NH_4Cl	100	7	0	7
10	DMSO/HFIP (9:1)	4CzIPN	None	100	trace	trace	trace

Lastly, several modifications were applied to the conditions identified along with running controls. No photocatalyst led to no product formation while no Hantzsch Ester led to very little (3%). Other modifications, such as increasing equivalents of Hantzsch Ester, 2-bromopyridine or tripSH did not improve yield. An equal mixture of MeOH and DMA was tested as the solvent after observing that in MeOH/H_2O the solution appeared cloudy. This led to lowered conversion (85%) and yield (5%).

Table 8. Optimization modifications and controls

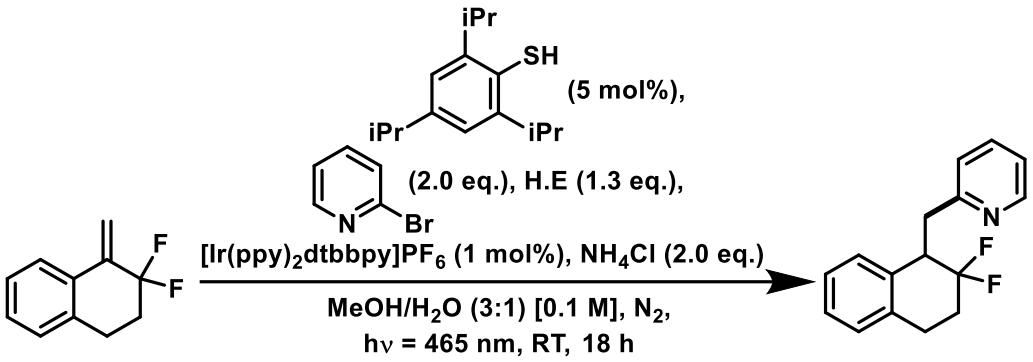

Entry	Modification	SM Conversion (%)	Yield X (%)	Yield Y (%)	X+Y (%)
1	No PC	15	0	0	0
2	MeOH/DMA (1:1) solvent	85	3	2	5
3	No H.E	15	3	0	3
4	3 eq. H.E	100	6	12	18
5	3 eq. 2-bromopyridine	98	5	14	19
6	10 mol% tripSH	93	7	9	16

Unfortunately, time constraints prevented further optimization and, due to currently poor yields, a scope could not be established. The competing β-F elimination pathway appears to be more favourable than anticipated, despite alterations from original conditions. Identification of the desired product has also proven difficult, as it is unknown why there are two products, which are difficult to separate and may be isomers. One hypothesis is that the desired product was successfully synthesized and exists as different atropisomers. Atropisomers are a form of chirality that arise from restricted rotation around a sigma bond (**Figure 13**).

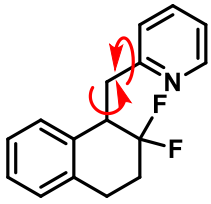

Figure 13. Red arrows depicting possible bonds with restricted rotation leading to atropisomerism

Atropisomers are known in biaryl systems as well as molecules featuring two aryl groups separated by a one-atom bridge, typical for oxygen, sulfur, nitrogen and boron, although other variations such as aromatic amides and aryl alkenes are known.[63-65] Upon attempted isolation (column conditions: 40% ethyl acetate/hexanes), the products X and Y co-eluted and a third set of peaks became visible in the ^{19}F NMR spectrum. Although, tri-axial and bi-axial atropisomerism exists, bi-axial atropisomerism would imply 4 distinct isomers which has not been observed.[66] In the original ^{19}F NMR spectrum, this peak was not visible as it has a very similar chemical shift to product Y whilst also appearing in smaller amounts than X or Y.

3.3 Proposed mechanism

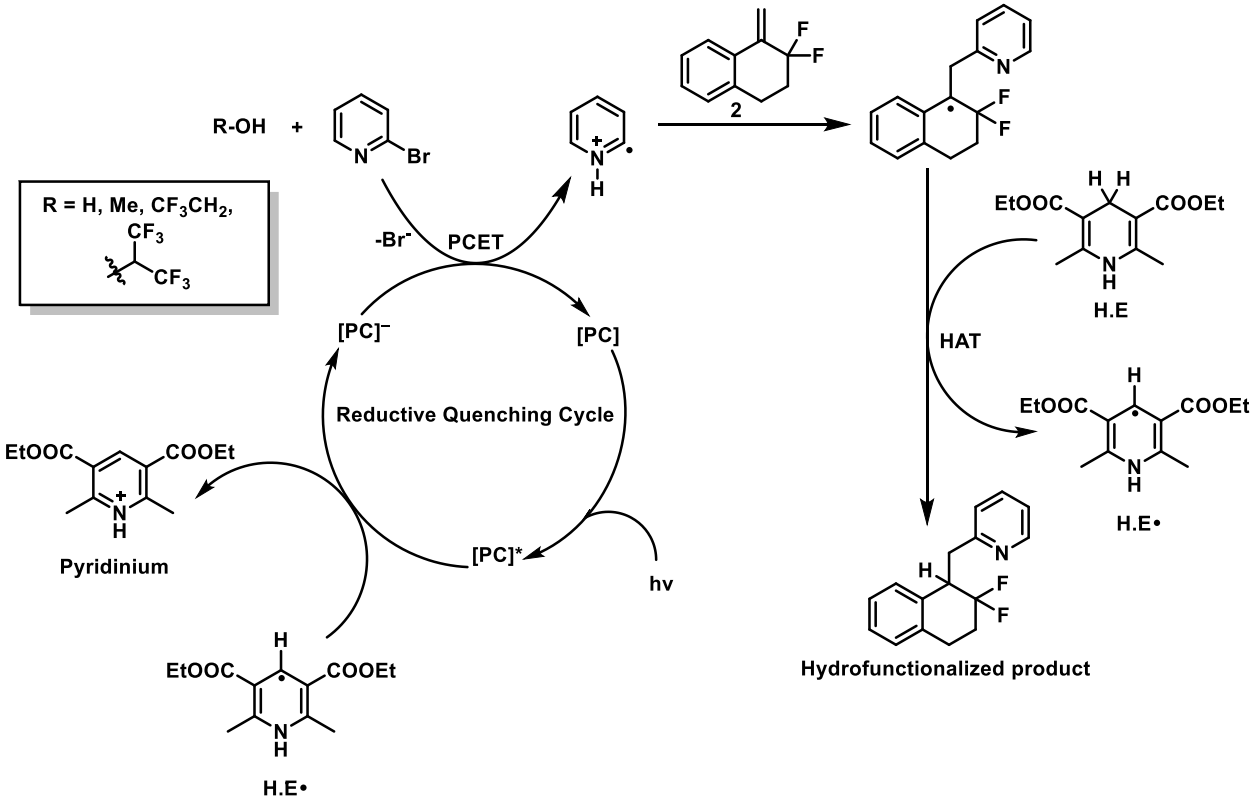

Scheme 9. Proposed mechanism for the heteroarylation of allylic difluoride **2**

2-Bromopyridinium has a pK_a of about 0.7, making 2-bromopyridine a weak base, thus it is unlikely a classic protonation event will occur initially.[67] Instead, it is proposed that 2-bromopyridine undergoes proton-coupled electron transfer (PCET), where a proton is likely transferred from a protic solvent and a single electron is transferred from $[PC]^-$, whilst losing bromide to generate a pyridinium radical.[57] It is unclear if the PCET event is concerted or stepwise, and if it is stepwise which step occurs first. This pyridinium

radical can react with allylic difluoride **2** to generate a carbon-centered radical α to the *gem*-difluoro group. This intermediate can then undergo hydrogen atom transfer from the Hantzsch ester to generate the final hydrofunctionalized product. The dihydropyridine radical can then be oxidized into a pyridinium by [PC]*.

4. Experimental

General Procedure for the reaction of allylic difluoride **2** and NHPI Ester (Method A/B)

Allylic difluoride **2** (36 mg, 0.20 mmol) was added to a 4-mL vial via pipette. In a second 4-mL vial, photocatalyst (if applicable, 0.002 mmol), NHPI ester (0.40 mmol) and Hantzsch Ester (76 mg, 0.30 mmol) were added. The allylic difluoride was transferred to the other vial by dissolving with the organic reaction solvent and transferring via syringe. A stir bar was added, the vial was capped with a septum cap, sealed with electrical tape and the vial was flushed with N_2 while stirring. After removing the N_2 inlet, the vial was promptly sealed by melting Parafilm wax over the punctures in the septum. The reaction mixture was then irradiated, while stirring, for 18 hours under blue light (465 nm, P = 3.50 W). To a 20-mL vial, NMR standard 2-fluoro-4-nitrotoluene (approx. 31 mg, 0.20 mmol) was added. A small amount of ethyl acetate was used to dissolve the standard. The reaction mixture was diluted with ethyl acetate, added to the 20-mL vial containing the internal standard solution, and quenched with saturated aqueous sodium bicarbonate. After vigorous shaking, an aliquot (roughly 90 µL) of the organic layer was taken and diluted with $CDCl_3$ before being taken for ^{19}F NMR analysis.

General Procedure for the reaction of allylic difluoride **2** and NHPI Ester (Method C)

Allylic difluoride **2** (36.0 mg, 0.200 mmol) was added to a 4-mL vial via pipette. In a second 4-mL vial, Eosin Y (13 mg, 0.02 mmol) and NHPI ester (0.40 mmol) were added. The allylic difluoride was then transferred to the other vial by dissolving with the organic reaction solvent and transferring via syringe. The vial was charged with DIPEA (69.7 µL, 0.40 mmol), a stir bar was added, the vial was capped with a septum cap, sealed with electrical tape and the vial was flushed with N_2 while stirring. After removing the N_2 inlet, the vial was promptly sealed by melting Parafilm wax over the punctures in the septum. The reaction mixture was then irradiated, while stirring, for 18 hours under green light (530 nm, P = 1.12 W). To a 20-mL vial, NMR standard 2-fluoro-4-nitrotoluene (approx. 31 mg, 0.20 mmol) was added. A small amount of ethyl

acetate was used to dissolve the standard. The reaction mixture was diluted with ethyl acetate, added to the 20-mL vial containing the internal standard solution, and quenched with saturated aqueous sodium bicarbonate. After vigorous shaking, an aliquot (roughly 90 μL) of the organic layer was taken and diluted with $CDCl_3$ before being taken for ^{19}F NMR analysis.

General Procedure for the reaction of allylic difluoride **2** and carboxylic acids (Method D)

Allylic difluoride **2** (36.0 mg, 0.200 mmol) was added to a 4-mL vial via pipette. In a second 4-mL vial, the photocatalyst (0.002 mmol), carboxylic acid (0.40 mmol), PPh_3 (79 mg, 0.30 mmol) and DMAP (5 mg, 0.02 mmol) were added to the vial. The allylic difluoride was then transferred to the other vial by dissolving with the organic reaction solvent and transferring via syringe. A stir bar was added, the vial was capped with a septum cap, sealed with electrical tape and the vial was flushed with N_2 while stirring. After removing the N_2 inlet, the vial was promptly sealed by melting Parafilm wax over the punctures in the septum. The reaction mixture was then irradiated, while stirring, for 18 hours under blue light (465 nm, P = 3.50 W). To a 20-mL vial, NMR standard 2-fluoro-4-nitrotoluene (approx. 31 mg, 0.20 mmol) was added. A small amount of ethyl acetate was used to dissolve the standard. The reaction mixture was diluted with ethyl acetate, added to the 20-mL vial containing the internal standard solution, and quenched with saturated aqueous sodium bicarbonate. After vigorous shaking, an aliquot (roughly 90 μL) of the organic layer was taken and diluted with $CDCl_3$ before being taken for ^{19}F NMR analysis.

General Procedure for the reaction of allylic difluoride **2** and 2-bromopyridine (Method E)

Version A – solid acid additive

Allylic difluoride **2** (36.0 mg, 0.200 mmol) was added to a 4-mL vial via pipette. In a second 4-mL vial, photocatalyst (0.002 mmol), Hantzsch Ester (65.9 mg, 0.26 mmol) and an acid additive (0.40 mmol) were added. The allylic difluoride was then transferred to the other vial by dissolving with the organic reaction solvent and transferring via syringe. If applicable, the second solvent was added (H_2O or HFIP). The vial was charged with 2-bromopyridine (38.1 μL, 0.400 mmol). If applicable, 2,4,6-triisopropylbenzenethiol (2.5 μL, 0.010 mmol) was added. A stir bar was added, the vial was capped with a septum cap, sealed with electrical tape and the vial was flushed with N_2 while stirring. After removing the N_2 inlet, the vial was promptly sealed by melting Parafilm wax over the punctures in the septum. The reaction mixture was then irradiated,

while stirring, for 18 hours under blue (465 nm, P = 3.50 W) or green (530 nm, P = 1.12 W) light. To a 20-mL vial, NMR standard 2-fluoro-4-nitrotoluene (approx. 31 mg, 0.20 mmol) was added. A small amount of ethyl acetate was used to dissolve the standard. The reaction mixture was diluted with ethyl acetate, added to the 20-mL vial containing the internal standard solution, and quenched with saturated aqueous sodium bicarbonate. After vigorous shaking, an aliquot (roughly 90 μL) of the organic layer was taken and diluted with $CDCl_3$ before being taken for ^{19}F NMR analysis.

Version B – liquid acid additive

Allylic difluoride **2** (36.0 mg, 0.200 mmol) was added to a 4-mL vial via pipette. In a second 4-mL vial, photocatalyst (0.002 mmol) and Hantzsch Ester (65.9 mg, 0.26 mmol) were added. The allylic difluoride was then transferred to the other vial by dissolving with the organic reaction solvent and transferring via syringe. If applicable, the second solvent was added (H_2O or HFIP). The acid additive (0.400 mmol) was added as an aqueous solution. The vial was charged with 2-bromopyridine (38.1 μL, 0.400 mmol). If applicable, 2,4,6-triisopropylbenzenethiol (2.5 μL, 0.010 mmol) was added. A stir bar was added, the vial was capped with a septum cap, sealed with electrical tape and the vial was flushed with N_2 while stirring. After removing the N_2 inlet, the vial was promptly sealed by melting Parafilm wax over the punctures in the septum. The reaction mixture was then irradiated, while stirring, for 18 hours under blue (465 nm, P = 3.50 W) or green (530 nm, P = 1.12 W) light. To a 20-mL vial, NMR standard 2-fluoro-4-nitrotoluene (approx. 31 mg, 0.20 mmol) was added. A small amount of ethyl acetate was used to dissolve the standard. The reaction mixture was diluted with ethyl acetate, added to the 20-mL vial containing the internal standard solution, and quenched with saturated aqueous sodium bicarbonate. After vigorous shaking, an aliquot (roughly 90 μL) of the organic layer was taken and diluted with $CDCl_3$ before being taken for ^{19}F NMR analysis.

Procedure for Synthesis of NHPI Ester: 1,3-dioxoisoindolin-2-yl benzoate

A magnetic stir bar was added to a 50-mL round-bottom flask along with benzoic acid (0.733 g, 6.00 mmol, *N*-hydroxyphthalamide (0.979 g, 6.00 mmol) and DMAP (0.103 g, 0.600 mmol). This was then dissolved with 24.0 mL of DCM followed by the addition of DIC (0.94 mL, 6.0 mmol). The reaction was allowed to react and was stirred at room temperature overnight. The crude solution was diluted with ethyl

acetate, washed with sat. Na_2CO_3 (x3) and then acidified/washed with 2.0 M HCl (x6). No further purification was required, and the product appeared as a white solid.

Procedure for Starting Material Synthesis – Allylic Difluoride **2**

A stir bar was added to a flask along with 24 mL of benzene, α-tetralone (1.60 mL, 12.0 mmol), 1-butylamine (1.42 mL, 14.4 mmol) and 6 drops of trifluoracetic acid. A Dean-Stark apparatus was then installed and wrapped in aluminium foil. The mixture was heated in an oil bath at 100 °C overnight during which the mixture went from colourless to yellow and clear. The benzene was evaporated under reduced pressure, and the crude intermediate imine product was dissolved in ethyl acetate. This solution was washed with sat. $NaHCO_{3(aq)}$ and washed with brine, then dried over Na_2SO_4, filtered and the solvent was evaporated under reduced pressure. The imine was then dissolved in 120 mL of acetonitrile in a flask containing a stir bar. To ensure anhydrous conditions, additional Na_2SO_4 was added (1.2 g, 100 mg/mmol), followed by Selectfluor (8.50 g, 24.0 mmol). The flask was placed under N_2 and stirred for 5 minutes at which point a condenser was installed and the mixture was heated in an oil bath at 85 °C overnight. After heating, the mixture was allowed to reach room temperature, at which point 0.6 mL conc. HCl and 10 mL H_2O were added. The solution was stirred and allowed to react for 10 minutes. The solvent was the evaporated under reduced pressure and the residue was subsequently diluted with ethyl acetate. It was then washed with saturated $NaHCO_{3(aq)}$ and washed with brine, then dried over Na_2SO_4, filtered and the solvent was evaporated under reduced pressure. The crude was purified via flash chromatography using 40% DCM in hexanes as the eluent.

Subsequently, a new flask was obtained to which a stir bar and dry THF (0.60 M) were added. Ph_3P-CH_3I (1.1 eq.) was added next. Then, the flask was placed under N_2 and cooled to 0 °C, via ice bath, after which HMDS (1.1 eq.) was added via syringe and *n*-butyllithium (1.1 eq.) was added dropwise. The reaction was then returned to room temperature and stirred for 30 minutes, to allow the formation of the ylide. The isolated 2,2-difluoro-1-tetralone product from the previous step (1 eq.) was added to a separate flask and dissolved in dry THF (0.16 M). The main reaction mixture, containing the ylide, was cooled to 0 °C and the 2,2-difluoro-1-tetralone solution was slowly added to the reaction mixture. The mixture was left in the ice bath and allowed to slowly reach room temperature, stirring under N_2 overnight. The mixture was diluted

with hexanes, then washed with saturated $NaHCO_3$, followed by brine. It was then dried over $MgSO_4$, filtered and the solvent was evaporated under reduced pressure. This crude product was purified via flash chromatography using hexanes as the eluent to give the allylic difluoride as a colourless oil.

Procedure for Synthesis of Methyltriphenylphosphonium Iodide

Triphenylphosphine (2.6229 g, 10.0 mmol) was added to a round-bottom flask and dissolved in 50 mL of toluene. After flushing the headspace with N_2, iodomethane (0.75 mL, 12.0 mmol) was added. The solution was stirred overnight, at room temperature. The resulting precipitate was filtered over a glass frit and washed with hexanes. The resulting white powder was dried under vacuum for several hours.

Procedure for crystal growth of difluoroketone **1**

Roughly 30 mg of difluoroketone **1** was added to a 4-mL vial. A minimum amount of hexanes was used to dissolve the solid. Then, the vial was loosely capped and left in the fridge for several days. Long, thin, needle-like crystals were observed near the bottom of the vial, along with powdered impurities. The crystals were collected and screened until a suitable single crystal was obtained for X-ray diffraction studies.

5. Crystallographic data

A suitable crystal was selected on a Rigaku SuperNova, Dual Cu/Mo, Pilatus 200K diffractometer. The crystal was kept at 99.97(18) K during data collection. Using Olex2, the structure was solved with the olex2.solve structure solution program and refined with the olex2.refine refinement package using Gauss-Newton minimisation.[68, 69]

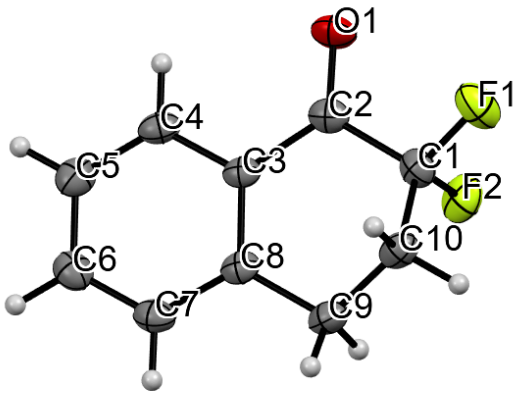

Figure 14. Crystal structure of 2,2-difluoro-3,4-dihydronaphthalen-1(2*H*)-one (**1**)

CCDC Deposition Number: 2555464, Refcode: RAPTAI

Table 9. Crystal data and structure refinement for 2,2-difluoro-3,4-dihydronaphthalen-1(2*H*)-one (**1**)

Identification code	2,2-difluoro-3,4-dihydronaphthalen-1(2H)-one
Empirical formula	$C_{10}H_8F_2O$
Formula weight	182.171
Temperature/K	99.97(18)
Crystal system	monoclinic
Space group	$P2_1/c$
a/Å	8.6733(4)
b/Å	16.3590(6)
c/Å	6.1741(3)
α/°	90
β/°	110.097(5)
γ/°	90
Volume/Å^3	822.68(7)
Z	4
ρ_{calc}g/cm^3	1.471
μ/mm^{-1}	1.073
F(000)	377.6
Crystal size/mm^3	0.460 × 0.091 × 0.05
Radiation	Cu Kα (λ = 1.54184)
2Θ range for data collection/°	10.82 to 161.02
Index ranges	-11 ≤ h ≤ 8, -20 ≤ k ≤ 20, -5 ≤ l ≤ 7
Reflections collected	5102
Independent reflections	1651 [R_{int} = 0.0266, R_{sigma} = 0.0283]
Data/restraints/parameters	1651/0/118
Goodness-of-fit on F^2	1.012
Final R indexes [I>=2σ (I)]	R_1 = 0.0398, wR_2 = 0.0934
Final R indexes [all data]	R_1 = 0.0468, wR_2 = 0.1075
Largest diff. peak/hole / e Å^{-3}	0.31/-0.27

Table 10. Fractional Atomic Coordinates (×10^4) and Equivalent Isotropic Displacement Parameters (Å^2×10^3) for 2,2-difluoro-3,4-dihydronaphthalen-1(2*H*)-one (**1**). U_{eq} is defined as 1/3 of the trace of the orthogonalised U_{IJ} tensor

Atom	*x*	*y*	*z*	U(eq)
F2	886.2(14)	5340.6(6)	3568.6(18)	39.6(3)
F1	−355.5(13)	6492.3(8)	2271.7(19)	43.3(3)
O1	1902.8(16)	6907.3(8)	6220(2)	33.3(3)
C3	4115(2)	6446.4(9)	5078(3)	23.3(3)
C8	4565(2)	6040.1(9)	3381(3)	24.8(3)
C4	5316(2)	6808.7(9)	6976(3)	27.6(4)
C2	2376(2)	6533.5(9)	4862(3)	25.7(3)
C10	1614(2)	6038.0(10)	703(3)	29.3(4)
C1	1112(2)	6106.5(10)	2796(3)	28.1(4)
C5	6951(2)	6778.2(10)	7180(3)	31.3(4)
C9	3300(2)	5634.0(10)	1342(3)	29.9(4)
C7	6222(2)	6019.1(10)	3623(3)	30.3(4)

C6	7402(2)	6386.8(10)	5500(3)	31.9(4)

Table 11. Anisotropic Displacement Parameters ($Å^2×10^3$) for 2,2-difluoro-3,4-dihydronaphthalen-1(2*H*)-one (**1**). The Anisotropic displacement factor exponent takes the form: $-2\pi^2[h^2a^{*2}U_{11}+2hka^*b^*U_{12}+\ldots]$

Atom	U_{11}	U_{22}	U_{33}	U_{12}	U_{13}	U_{23}
F2	48.6(6)	33.3(6)	40.0(6)	−15.1(5)	19.2(5)	3.4(4)
F1	30.3(6)	63.4(8)	36.4(6)	9.3(5)	11.4(5)	5.8(5)
O1	40.9(7)	34.8(7)	31.5(6)	3.5(5)	22.0(5)	−0.1(5)
C3	31.1(8)	17.6(7)	23.3(7)	1.8(6)	12.2(6)	2.4(5)
C8	35.1(8)	16.9(7)	25.1(7)	−0.4(6)	13.6(6)	2.5(5)
C4	38.8(9)	21.4(7)	23.4(7)	3.8(7)	11.7(7)	0.8(6)
C2	34.6(9)	21.8(7)	24.6(7)	2.1(6)	15.1(7)	5.2(6)
C10	36.7(9)	28.5(8)	23.4(7)	−4.3(7)	11.3(7)	−0.9(6)
C1	28.9(8)	27.1(8)	30.2(8)	−0.6(6)	12.8(7)	4.6(6)
C5	34.0(9)	25.6(8)	30.0(8)	2.7(7)	5.4(7)	2.8(6)
C9	40.0(9)	23.8(8)	28.8(8)	−4.3(7)	15.4(7)	−4.7(6)
C7	37.1(9)	23.6(8)	34.5(9)	3.8(7)	17.8(7)	1.5(6)
C6	30.6(8)	27.2(8)	39.3(9)	3.7(7)	13.7(7)	6.3(7)

Table 12. Bond Lengths for 2,2-difluoro-3,4-dihydronaphthalen-1(2*H*)-one (**1**)

Atom	Atom	Length/Å	Atom	Atom	Length/Å
F2	C1	1.3786(19)	C8	C7	1.393(2)
F1	C1	1.357(2)	C4	C5	1.380(3)
O1	C2	1.217(2)	C2	C1	1.535(2)
C3	C8	1.405(2)	C10	C1	1.503(2)
C3	C4	1.404(2)	C10	C9	1.528(2)
C3	C2	1.474(2)	C5	C6	1.385(3)
C8	C9	1.510(2)	C7	C6	1.392(2)

Table 13. Bond Angles for 2,2-difluoro-3,4-dihydronaphthalen-1(2*H*)-one (**1**)

Atom	Atom	Atom	Angle/˚	Atom	Atom	Atom	Angle/˚
C4	C3	C8	120.35(15)	F1	C1	F2	105.78(13)
C2	C3	C8	121.08(14)	C2	C1	F2	105.77(12)
C2	C3	C4	118.51(14)	C2	C1	F1	109.27(14)
C9	C8	C3	121.40(15)	C10	C1	F2	110.34(14)
C7	C8	C3	118.22(15)	C10	C1	F1	110.78(14)
C7	C8	C9	120.38(15)	C10	C1	C2	114.44(14)
C5	C4	C3	120.36(15)	C6	C5	C4	119.60(16)
C3	C2	O1	124.25(15)	C10	C9	C8	112.46(14)
C1	C2	O1	119.18(15)	C6	C7	C8	120.98(16)
C1	C2	C3	116.56(14)	C7	C6	C5	120.47(16)
C9	C10	C1	110.13(14)				

Table 14. Torsion Angles for 2,2-difluoro-3,4-dihydronaphthalen-1(2*H*)-one (**1**)

A	B	C	D	Angle/˚	A	B	C	D	Angle/˚
F2	C1	C2	O1	-87.54(14)	C8	C3	C2	C1	4.27(16)
F2	C1	C2	C3	91.47(13)	C8	C9	C10	C1	-51.61(15)
F2	C1	C10	C9	-65.51(14)	C8	C7	C6	C5	0.43(19)
F1	C1	C2	O1	25.91(15)	C4	C3	C8	C9	179.03(14)
F1	C1	C2	C3	-155.07(12)	C4	C3	C8	C7	-0.91(17)
F1	C1	C10	C9	177.69(14)	C4	C3	C2	C1	-178.34(14)
O1	C2	C3	C8	-176.78(16)	C4	C5	C6	C7	-0.57(19)
O1	C2	C3	C4	0.61(19)	C2	C3	C8	C9	-3.62(17)
O1	C2	C1	C10	150.79(15)	C2	C3	C8	C7	176.43(15)
C3	C8	C9	C10	27.81(16)	C2	C3	C4	C5	-176.62(14)
C3	C8	C7	C6	0.31(17)	C2	C1	C10	C9	53.62(14)
C3	C4	C5	C6	-0.04(18)	C10	C9	C8	C7	-152.25(14)
C3	C2	C1	C10	-30.20(15)	C9	C8	C7	C6	-179.64(15)
C8	C3	C4	C5	0.79(17)					

Table 15. Hydrogen Atom Coordinates (Å×10^4) and Isotropic Displacement Parameters (Å^2×10^3) for 2,2-difluoro-3,4-dihydronaphthalen-1(2*H*)-one (**1**)

Atom	*x*	*y*	*z*	U(eq)
H4	5002(2)	7076.3(9)	8126(3)	33.1(4)
H10a	794(2)	5708.9(10)	-493(3)	35.1(4)
H10b	1653(2)	6589.2(10)	61(3)	35.1(4)
H5	7761(2)	7024.1(10)	8466(3)	37.6(5)
H9a	3675(2)	5657.5(10)	-1(3)	35.9(4)
H9b	3204(2)	5051.2(10)	1709(3)	35.9(4)
H7	6551(2)	5749.7(10)	2490(3)	36.4(5)
H6	8525(2)	6369.3(10)	5629(3)	38.3(5)

Crystal Data for $C_{10}H_8F_2O$ (*M* =182.171 g/mol): monoclinic, space group $P2_1/c$ (no. 14), *a* = 8.6733(4) Å, *b* = 16.3590(6) Å, *c* = 6.1741(3) Å, *β* = 110.097(5)°, *V* = 822.68(7) Å^3, *Z* = 4, *T* = 99.97(18) K, μ(Cu Kα) = 1.073 mm^{-1}, *Dcalc* = 1.471 g/cm^3, 5102 reflections measured (10.82° ≤ 2Θ ≤ 161.02°), 1651

unique (R_{int} = 0.0266, R_{sigma} = 0.0283) which were used in all calculations. The final R_1 was 0.0398 (I>=2u(I)) and wR_2 was 0.1075 (all data).

Refinement model description

Number of restraints - 0, number of constraints - 14.

Details:

1. Fixed Uiso

At 1.2 times of:

All C(H) groups, All C(H,H) groups

2.a Secondary CH2 refined with riding coordinates:

C10(H10a,H10b), C9(H9a,H9b)

2.b Aromatic/amide H refined with riding coordinates:

C4(H4), C5(H5), C7(H7), C6(H6)

6. Conclusion and future outlook

The photocatalytic hydrofunctionalization of allylic difluoride **2** was attempted in an effort to functionalize compounds bearing *gem*-difluoro groups, useful groups in pharmaceuticals and agrochemicals, with other pharmaceutically and agrochemically relevant motifs. First, allylic difluoride **2** was synthesized following established procedures. Difluoroketone **1**, the precursor to **2**, was analyzed via single x-ray diffractometry. From among hydrofunctionalization methods surveyed from literature, the system using halopyridines as radical precursors showed the most promise and was chosen for further investigation. A multitude of solvent and photocatalyst combinations were tested, along with testing the effects of acid additives and a HAT catalyst. Unexpectedly, several sets of peaks matched the description expected for the product; one possible, yet unconfirmed, cause for this is atropisomerism. It is proposed that, in the future, different kinds of halopyridines are tested as radical precursors, such as 2-bromo-6-methylpyridine and other related structures. Other allylic difluorides should also be explored as substrates for hydrofunctionalization. Specifically, it would be interesting to test an allylic difluoride with an electron-deficient naphthalene core as well as testing an acylic version of the allylic difluoride **2**. Although Hantzsch esters should be potent H· sources and participate readily in SET, other sources should be tested such as other Hantzsch ester derivatives or silicon-based reagents such as tris(trimethylsilyl)silane. It would be

interesting to see if the system requires an input of thermal energy to overcome the activation energy towards more successful hydrofunctionalization. Overall, there is much to still be developed regarding the heteroarylation, and more generally hydrofunctionalization, of allylic difluorides, however, facile access to *gem*-difluorinated compounds bonded to industrially abundant and popular motifs such as *N*-heterocycles continues to be desirable.

7. References

(1) Tantardini, C.; Oganov, A. R. Thermochemical electronegativities of the elements. *Nat. Commun.* **2021**, *12* (1), 2087. DOI: 10.1038/s41467-021-22429-0.
(2) Bondi, A. van der Waals Volumes and Radii. *The Journal of Physical Chemistry* **1964**, *68* (3), 441–451. DOI: 10.1021/j100785a001.
(3) Blanksby, S. J.; Ellison, G. B. Bond Dissociation Energies of Organic Molecules. *Acc. Chem. Res.* **2003**, *36* (4), 255–263. DOI: 10.1021/ar020230d.
(4) Dehnen, S.; Schafer, L. L.; Lectka, T.; Togni, A. Fluorine: A Very Special Element and Its Very Special Impacts on Chemistry. *J. Org. Chem.* **2021**, *86* (23), 16213–16219. DOI: 10.1021/acs.joc.1c02745.
(5) Hagmann, W. K. The Many Roles for Fluorine in Medicinal Chemistry. *J. Med. Chem.* **2008**, *51* (15), 4359–4369. DOI: 10.1021/jm800219f.
(6) O'Neill, P. M.; Harrison, A. C.; Storr, R. C.; Hawley, S. R.; Ward, S. A.; Park, B. K. The Effect of Fluorine Substitution on the Metabolism and Antimalarial Activity of Amodiaquine. *J. Med. Chem.* **1994**, *37* (9), 1362–1370. DOI: 10.1021/jm00035a017.
(7) Mei, H.; Han, J.; Fustero, S.; Medio-Simon, M.; Sedgwick, D. M.; Santi, C.; Ruzziconi, R.; Soloshonok, V. A. Fluorine-Containing Drugs Approved by the FDA in 2018. *Chem. Eur. J.* **2019**, *25* (51), 11797–11819. DOI: 10.1002/chem.201901840.
(8) Mei, H.; Remete, A. M.; Zou, Y.; Moriwaki, H.; Fustero, S.; Kiss, L.; Soloshonok, V. A.; Han, J. Fluorine-containing drugs approved by the FDA in 2019. *Chin. Chem. Lett* **2020**, *31* (9), 2401–2413. DOI: 10.1016/j.cclet.2020.03.050.
(9) Yu, Y.; Liu, A.; Dhawan, G.; Mei, H.; Zhang, W.; Izawa, K.; Soloshonok, V. A.; Han, J. Fluorine-containing pharmaceuticals approved by the FDA in 2020: Synthesis and biological activity. *Chin. Chem. Lett* **2021**, *32* (11), 3342–3354. DOI: 10.1016/j.cclet.2021.05.042.
(10) He, J.; Li, Z.; Dhawan, G.; Zhang, W.; Sorochinsky, A. E.; Butler, G.; Soloshonok, V. A.; Han, J. Fluorine-containing drugs approved by the FDA in 2021. *Chin. Chem. Lett* **2023**, *34* (1), 107578. DOI: 10.1016/j.cclet.2022.06.001.
(11) Wang, N.; Mei, H.; Dhawan, G.; Zhang, W.; Han, J.; Soloshonok, V. A. New Approved Drugs Appearing in the Pharmaceutical Market in 2022 Featuring Fragments of Tailor-Made Amino Acids and Fluorine. *Molecules* **2023**, *28* (9), 3651. DOI: 10.3390/molecules28093651.
(12) Wang, Q.; Bian, Y.; Dhawan, G.; Zhang, W.; Sorochinsky, A. E.; Makarem, A.; Soloshonok, V. A.; Han, J. FDA approved fluorine-containing drugs in 2023. *Chin. Chem. Lett* **2024**, *35* (11), 109780. DOI: 10.1016/j.cclet.2024.109780.
(13) Du, Y.; Bian, Y.; Baecker, D.; Dhawan, G.; Semghouli, A.; Kiss, L.; Zhang, W.; Sorochinsky, A. E.; Soloshonok, V. A.; Han, J. Fluorine in the Pharmaceutical Industry: FDA-Approved Fluorine-Containing Drugs in 2024. *Chem. Eur. J.* **2025**, *31* (25), e202500662. DOI: 10.1002/chem.202500662.
(14) Mishra, S.; Jadala, C.; Cardoza, S.; Potuganti, G. R.; Velma, G. R. Fluorine-containing FDA-approved small-molecule drugs in 2025: significance, synthetic insights, and therapeutic applications. *RSC Adv.* **2026**, *16* (15), 13830–13850. DOI: 10.1039/D6RA01711H.
(15) Bertoch, T.; D'Aunno, D.; McCoun, J.; Solanki, D.; Taber, L.; Urban, J.; Oswald, J.; Swisher, M. W.; Tian, S.; Miao, X.; et al. Suzetrigine, a Nonopioid NaV1.8 Inhibitor for Treatment of Moderate-to-severe Acute Pain: Two Phase 3 Randomized Clinical Trials. *Anesthesiology* **2025**, *142* (6), 1085–1099. DOI: 10.1097/aln.0000000000005460.
(16) Turner Nicholas, C.; Im, S.-A.; Saura, C.; Juric, D.; Loibl, S.; Kalinsky, K.; Schmid, P.; Loi, S.; Sunpaweravong, P.; Musolino, A.; et al. Inavolisib-Based Therapy in PIK3CA-Mutated Advanced Breast

Cancer. *N. Eng. J. Med.* **2024**, *391* (17), 1584–1596. DOI: 10.1056/NEJMoa2404625 (accessed 2026/04/16).
(17) Gerhart, J.; Cox, D. S.; Singh, R. S. P.; Chan, P. L. S.; Rao, R.; Allen, R.; Shi, H.; Masters, J. C.; Damle, B. A Comprehensive Review of the Clinical Pharmacokinetics, Pharmacodynamics, and Drug Interactions of Nirmatrelvir/Ritonavir. *Clin. Pharmacokinet.* **2024**, *63* (1), 27–42. DOI: 10.1007/s40262-023-01339-y.
(18) Ogawa, Y.; Tokunaga, E.; Kobayashi, O.; Hirai, K.; Shibata, N. Current Contributions of Organofluorine Compounds to the Agrochemical Industry. *iScience* **2020**, *23* (9), 101467. DOI: 10.1016/j.isci.2020.101467.
(19) Patel, A. A.; Cahill, K.; Saygin, C.; Odenike, O. Cedazuridine/decitabine: from preclinical to clinical development in myeloid malignancies. *Blood. Adv.* **2021**, *5* (8), 2264–2271. DOI: 10.1182/bloodadvances.2020002929 From NLM.
(20) Xiu, Q.; Yin, X.; Chen, Y.; Zhang, Z.; Mao, Y.; Wang, T.; Zhang, J.; Zhou, M.; Duan, Y. Action mechanism of a novel agrichemical quinofumelin against Fusarium graminearum. *eLife* **2025**, *14*, RP105892. DOI: 10.7554/eLife.105892.
(21) Hasek, W. R.; Smith, W. C.; Engelhardt, V. A. The Chemistry of Sulfur Tetrafluoride. II. The Fluorination of Organic Carbonyl Compounds1. *J. Am. Chem. Soc.* **1960**, *82* (3), 543–551. DOI: 10.1021/ja01488a012.
(22) Beaulieu, F.; Beauregard, L.-P.; Courchesne, G.; Couturier, M.; LaFlamme, F.; L'Heureux, A. Aminodifluorosulfinium Tetrafluoroborate Salts as Stable and Crystalline Deoxofluorinating Reagents. *Org. Lett.* **2009**, *11* (21), 5050–5053. DOI: 10.1021/ol902039q.
(23) Cochran, J. Letters - Labratory Explosion. *Chem. Eng. News* **1979**, *57* (12), 4–74. DOI: 10.1021/cen-v057n012.p004.
(24) Lal, G. S.; Pez, G. P.; Pesaresi, R. J.; Prozonic, F. M.; Cheng, H. Bis(2-methoxyethyl)aminosulfur Trifluoride: A New Broad-Spectrum Deoxofluorinating Agent with Enhanced Thermal Stability. *J. Org. Chem.* **1999**, *64* (19), 7048–7054. DOI: 10.1021/jo990566+.
(25) Mohammadkhani, L.; Heravi, M. M. XtalFluor-E: A useful and versatile reagent in organic transformations. *J. Fluorine Chem.* **2019**, *225*, 11–20. DOI: 10.1016/j.jfluchem.2019.06.006.
(26) Bloom, S.; Scerba, M. T.; Erb, J.; Lectka, T. Tricomponent Catalytic α,α-Difluorination of Acid Chlorides. *Org. Lett.* **2011**, *13* (19), 5068–5071. DOI: 10.1021/ol2019295.
(27) Tius, M. A. Xenon difluoride in synthesis. *Tetrahedron* **1995**, *51* (24), 6605–6634. DOI: 10.1016/0040-4020(95)00362-C.
(28) Umemoto, T.; Tomita, K. N-fluoropyridinium triflate and its derivatives - useful fluorinating agents. *J. Fluorine Chem.* **1987**, *35* (1), 14. DOI: 10.1016/0022-1139(87)95009-3.
(29) Differding, E.; Ofner, H. N-Fluorobenzenesulfonimide: A Practical Reagent For Electrophilic Fluorinations. *Synlett* **1991**, *1991* (3), 187–189. DOI: 10.1055/s-1991-20673.
(30) Nyffeler, P. T.; Durón, S. G.; Burkart, M. D.; Vincent, S. P.; Wong, C.-H. Selectfluor: Mechanistic Insight and Applications. *Angew. Chem. Int. Ed.* **2005**, *44* (2), 192–212. DOI: 10.1002/anie.200400648.
(31) Duchemin, N.; Buccafusca, R.; Daumas, M.; Ferey, V.; Arseniyadis, S. A Unified Strategy for the Synthesis of Difluoromethyl- and Vinylfluoride-Containing Scaffolds. *Org. Lett.* **2019**, *21* (20), 8205–8210. DOI: 10.1021/acs.orglett.9b02887.
(32) Fujiwara, Y.; Dixon, J. A.; Rodriguez, R. A.; Baxter, R. D.; Dixon, D. D.; Collins, M. R.; Blackmond, D. G.; Baran, P. S. A New Reagent for Direct Difluoromethylation. *J. Am. Chem. Soc.* **2012**, *134* (3), 1494–1497. DOI: 10.1021/ja211422g.
(33) Fuchigami, T.; Inagi, S. Recent Advances in Electrochemical Systems for Selective Fluorination of Organic Compounds. *Acc. Chem. Res.* **2020**, *53* (2), 322–334. DOI: 10.1021/acs.accounts.9b00520.
(34) Zhang, Z.-Q.; Wang, C.-Q.; Li, L.-J.; Piper, J. L.; Peng, Z.-H.; Ma, J.-A.; Zhang, F.-G.; Wu, J. Programmable synthesis of difluorinated hydrocarbons from alkenes through a photocatalytic linchpin strategy. *Chem. Sci.* **2023**, *14* (41), 11546–11553. DOI: 10.1039/D3SC03951J.
(35) Pravst, I.; Zupan, M.; Stavber, S. Efficient Synthesis of α,α-Difluoro Ketones Using SelectfluorTM F-TEDA-BF4. *Synthesis* **2005**, *2005* (18), 3140–3146. DOI: 10.1055/s-2005-918424.
(36) Semeniuk, T.; Challenger, J.; Dudas, T.; Toporkov, D.; van Hoeve, M. D.; Hamel, J.-D. Photoredox Decarboxylative 3-Fluoroallylation of α-Amino Acids. *Eur. J. Org. Chem.* **2025**, *28* (33), e202500519. DOI: 10.1002/ejoc.202500519.
(37) Landelle, G.; Bergeron, M.; Turcotte-Savard, M.-O.; Paquin, J.-F. Synthetic approaches to monofluoroalkenes. *Chem. Soc. Rev.* **2011**, *40* (5), 2867–2908. DOI: 10.1039/C0CS00201A.
(38) Bergeron, M.; Johnson, T.; Paquin, J.-F. The Use of Fluoride as a Leaving Group: SN2′ Displacement of a C-F Bond on 3,3-Difluoropropenes with Organolithium Reagents To Give Direct Access to Monofluoroalkenes. *Angew. Chem. Int. Ed.* **2011**, *50* (47), 11112–11116. DOI: 10.1002/anie.201105138.

(39) Pigeon, X.; Bergeron, M.; Barabé, F.; Dubé, P.; Frost, H. N.; Paquin, J.-F. Activation of Allylic C-F bonds: Palladium-Catalyzed Allylic Amination of 3,3-Difluoropropenes. *Angew. Chem. Int. Ed.* **2010**, *49* (6), 1123–1127. DOI: 10.1002/anie.200904747.
(40) Hamel, J.-D.; Drouin, M.; Paquin, J.-F. Synthesis of monofluoroalkenes using a Pt-catalyzed amination reaction of cyclic 3,3-difluoropropenes with secondary aliphatic amines. *J. Fluorine Chem.* **2015**, *174*, 81–87. DOI: 10.1016/j.jfluchem.2014.07.012.
(41) Shu, B.; Chen, S.-Y.; Deng, N.-X.; Zheng, T.; Xie, H.; Xie, X.-L.; Wu, J.-Q.; Cao, H.; Zhang, S.-S. Rhodium(iii)-catalyzed C–H/C–F activation sequence: expedient and divergent synthesis of 2-benzylated indoles and 2,2′-bis(indolyl)methanes. *Org. Chem. Front.* **2021**, *8* (16), 4445–4451. DOI: 10.1039/D1QO00462J.
(42) Semeniuk, T.; Dudas, T.; Okeh, E.; Felesky, T.; Hamel, J.-D. Photocatalytic Defluorinative α-Aminoalkylation of Allylic Difluorides. *J. Org. Chem.* **2024**, *89* (18), 13669–13677. DOI: 10.1021/acs.joc.4c01861.
(43) Semeniuk, T.; Toporkov, D. D.; de Goede, T.; Hamel, J.-D. Organophotocatalytic defluorinative γ-substitution towards monofluoroalkenes. *J. Flour. Chem* **2026**, *290*, 110540. DOI: 10.1016/j.jfluchem.2026.110540.
(44) Zhang, L.; Yu, X.; Ouyang, S.; Zhu, C.; Li, W.; Xie, J. Synthesis of β-Trifluoromethylated Ketones by Photocatalyzed Deoxygenative Coupling of Aromatic Acids with α-CF3-Substituted Styrenes. *Eur. J. Org. Chem.* **2024**, *27* (28), e202400392. DOI: 10.1002/ejoc.202400392.
(45) Wang, G.-Z.; Shang, R.; Cheng, W.-M.; Fu, Y. Decarboxylative 1,4-Addition of α-Oxocarboxylic Acids with Michael Acceptors Enabled by Photoredox Catalysis. *Org. Lett.* **2015**, *17* (19), 4830–4833. DOI: 10.1021/acs.orglett.5b02392.
(46) Zhang, M.; Ruzi, R.; Xi, J.; Li, N.; Wu, Z.; Li, W.; Yu, S.; Zhu, C. Photoredox-Catalyzed Hydroacylation of Olefins Employing Carboxylic Acids and Hydrosilanes. *Org. Lett.* **2017**, *19* (13), 3430–3433. DOI: 10.1021/acs.orglett.7b01391.
(47) Schwarz, J.; König, B. Metal-free, visible-light-mediated, decarboxylative alkylation of biomass-derived compounds. *Green Chem.* **2016**, *18* (17), 4743–4749. DOI: 10.1039/C6GC01101B.
(48) Chen, M.; Wang, C.; Xie, L.; Mao, T.; Xiao, L.; Wang, Z.; Han, W.-Y.; Liu, P.; Jia, J. Photo-induced decarboxylative coupling reaction between aliphatic N-hydroxyphthalimide esters and terminal 2-trifluoromethylalkenes. *Org. Biomol. Chem.* **2025**, *23* (10), 2445–2449. DOI: 10.1039/D4OB01950D.
(49) Li, R.; Yin, S.; Xie, L.; Li, X.; Jia, J.; Zhao, L.; He, C.-Y. Catalyst-free decarboxylative cross-coupling of N-hydroxyphthalimide esters with tert-butyl 2-(trifluoromethyl)acrylate and its application. *Org. Biomol. Chem.* **2024**, *22* (11), 2279–2283. DOI: 10.1039/D3OB02103C.
(50) Aycock, R. A.; Wang, H.; Jui, N. T. A mild catalytic system for radical conjugate addition of nitrogen heterocycles. *Chem. Sci.* **2017**, *8* (4), 3121–3125. DOI: 10.1039/C7SC00243B.
(51) Fan, P.; Zhang, C.; Lan, Y.; Lin, Z.; Zhang, L.; Wang, C. Photocatalytic hydroacylation of trifluoromethyl alkenes. *Chem. Commun.* **2019**, *55* (84), 12691–12694. DOI: 10.1039/C9CC07285C.
(52) Selvakumar, S.; Kang, Q.-K.; Arumugam, N.; Almansour, A. I.; Kumar, R. S.; Maruoka, K. Hypervalent iodine(III) catalyzed radical hydroacylation of chiral alkylidenemalonates with aliphatic aldehydes under photolysis. *Tetrahedron* **2017**, *73* (40), 5841–5846. DOI: 10.1016/j.tet.2017.08.018.
(53) Martínez-Balart, P.; Velasco-Rubio, Á.; Barbeira-Arán, S.; Jiménez-Cristóbal, H.; Fañanás-Mastral, M. Chemodivergent alkylation of trifluoromethyl alkenes via photocatalytic coupling with alkanes. *Green Chem.* **2024**, *26* (22), 11196–11205. DOI: 10.1039/D4GC04176C.
(54) Ji, C.-L.; Lu, Y.-N.; Xia, S.; Zhu, C.; Zhu, C.; Li, W.; Xie, J. Photoinduced Late-Stage Radical Decarboxylative and Deoxygenative Coupling of Complex Carboxylic Acids and Their Derivatives. *Angew. Chem. Int. Ed.* **2025**, *64* (9), e202423113. DOI: 10.1002/anie.202423113.
(55) Heravi, M. M.; Zadsirjan, V. Prescribed drugs containing nitrogen heterocycles: an overview. *RSC Adv.* **2020**, *10* (72), 44247–44311. DOI: 10.1039/D0RA09198G.
(56) Semeniuk, T.; Pounder, A.; Toporkov, D. D.; Wetmore, S. D.; Hamel, J.-D. Chemoselective Divergence via Substrate Control: Decarboxylative and Decarbonylative Coupling of 2-Oxoacids with Allylic Difluorides. *Eur. J. Org. Chem.* **2026**, *29* (1), e202501058. DOI: 10.1002/ejoc.202501058.
(57) Seath, C. P.; Vogt, D. B.; Xu, Z.; Boyington, A. J.; Jui, N. T. Radical Hydroarylation of Functionalized Olefins and Mechanistic Investigation of Photocatalytic Pyridyl Radical Reactions. *J. Am. Chem. Soc.* **2018**, *140* (45), 15525–15534. DOI: 10.1021/jacs.8b10238.

(58) Ruyet, L.; Roblick, C.; Häfliger, J.; Wang, Z.-X.; Stoffels, T. J.; Daniliuc, C. G.; Gilmour, R. Catalytic Ring Expanding Difluorination: An Enantioselective Platform to Access β,β-Difluorinated Carbocycles. *Angew. Chem. Int. Ed.* **2024**, *63* (22), e202403957. DOI: 10.1002/anie.202403957.
(59) Vogt, D. B.; Seath, C. P.; Wang, H.; Jui, N. T. Selective C–F Functionalization of Unactivated Trifluoromethylarenes. *J. Am. Chem. Soc.* **2019**, *141* (33), 13203–13211. DOI: 10.1021/jacs.9b06004.
(60) Semeniuk, T.; Toporkov, D. D.; de Goede, T.; Hamel, J.-D. Organophotocatalytic defluorinative γ-substitution towards monofluoroalkenes. *J. Fluor. Chem.* **2026**, *290*, 110540. DOI: 10.1016/j.jfluchem.2026.110540.
(61) Yang, H.; Liao, Y.; Guo, H.; Wang, M. Emerging Applications of Thiol-Based Catalysts in Hydrogen Atom Transfer Reactions: A Comprehensive Review. *Molecules* **2025**, *30* (20), 4058. DOI: 10.3390/molecules30204058.
(62) Motiwala, H. F.; Armaly, A. M.; Cacioppo, J. G.; Coombs, T. C.; Koehn, K. R. K.; Norwood, V. M. I. V.; Aubé, J. HFIP in Organic Synthesis. *Chem. Rev.* **2022**, *122* (15), 12544–12747. DOI: 10.1021/acs.chemrev.1c00749.
(63) Naghim, A.; Rodriguez, J.; Chuzel, O.; Chouraqui, G.; Bonne, D. Enantioselective Synthesis of Heteroatom-Linked Non-Biaryl Atropisomers. *Angew. Chem. Int. Ed.* **2024**, *63* (30), e202407767. DOI: 10.1002/anie.202407767.
(64) Birepinte, M.; Robert, F.; Pinet, S.; Chabaud, L.; Pucheault, M. Non-biaryl atropisomerism at the C–B bond in sterically hindered aminoarylboranes. *Org. Biomol. Chem.* **2020**, *18* (16), 3007–3011. DOI: 10.1039/D0OB00421A.
(65) Cheng, J. K.; Xiang, S.-H.; Li, S.; Ye, L.; Tan, B. Recent Advances in Catalytic Asymmetric Construction of Atropisomers. *Chem. Rev.* **2021**, *121* (8), 4805–4902. DOI: 10.1021/acs.chemrev.0c01306.
(66) Du, Y.-B.; Lu, Q.-T.; Cui, Y.-S.; Wu, K.-W.; Wang, Y.; Zhang, Y.-Z.; Zhao, Z.; Hou, J.-L.; Cai, Q. Enantioselective Synthesis of Atropisomeric Tri-Axis Naphthalenes via Diels–Alder Reaction and Dehydrative Aromatization of Isobenzofurans. *Angew. Chem. Int. Ed.* **2025**, *64* (10), e202421060. DOI: 10.1002/anie.202421060.
(67) Linnell, R. Notes- Dissociation Constants of 2-Substituted Pyridines. *J. Org. Chem.* **1960**, *25* (2), 290–290. DOI: 10.1021/jo01072a623.
(68) Dolomanov, O.; Bourhis, L.; Gildea, R.; Howard, J.; Puschmann, H. OLEX2: A complete structure solution, refinement and analysis program. *J. Appl. Crystallogr.* **2009**, *42*, 339–341. DOI: 10.1107/S0021889808042726.
(69) Bourhis, L. J.; Dolomanov, O. V.; Gildea, R. J.; Howard, J. A.; Puschmann, H. The anatomy of a comprehensive constrained, restrained refinement program for the modern computing environment - Olex2 dissected. *Acta Crystallogr. A* **2015**, *71* (Pt 1), 59–75. DOI: 10.1107/s2053273314022207.